

Supporting Information

Synergy of light harvesting and energy transfer as well as short-range charge shift reactions in multicomponent conjugates

Ettore Fazio,¹ Kim A. Winterfeld,² A. López-Pérez,¹ Tomás Torres*^{1,3,4} Dirk M. Guldi,*² Gema de la Torre,*^{1,3}

¹ Departamento de Química Orgánica, Universidad Autónoma de Madrid, C/ Francisco Tomás y Valiente 7, 28049-Madrid,

² Department of Chemistry and Pharmacy, Interdisciplinary Center for Molecular Materials (ICMM), Friedrich-Alexander-Universität Erlangen-Nürnberg, Egerlandstr. 3, 91058 Erlangen, Germany

³ Institute for Advanced Research in Chemical Sciences (IAdChem), Universidad Autónoma de Madrid, 28049 Madrid, Spain

⁴ IMDEA Nanociencia, C/Faraday, 9, Cantoblanco, 28049 Madrid, Spain

KEYWORDS: *phthalocyanine, subphthalocyanine, porphyrin, photosynthetic model, photo-induced charge separation*

1. *Material and general methods*

2. *Synthetic procedures*

3. *Characterization*

1. *Material and general methods*

Chemicals were purchased from commercial suppliers and used without further purification. Column chromatography was carried out on silica gel (Merck, Kieselgel 60, 230–400 mesh, 60 Å) and TLC was carried out on aluminium sheets pre-coated with silica gel 60 F254 (Merck). “Synthetic grade” solvents were used for chemical reactions and column chromatography purifications, and “anhydrous grade” for reactions under dry conditions. Additionally, THF was further dried by distillation with Na/benzophenone. NMR spectra were recorded on a Bruker AC-300 or a Bruker AC-500 instrument. Spectroscopic grade solvents were used for spectroscopic measurements. UV-Vis spectra were recorded employing a JASCO-V660 UV-Vis spectrophotometer. Fluorescence studies were carried out with a JASCO-V8600 fluorometer. Low resolution ESI-MS spectra were acquired using either a Thermo LTQ-XL linear ion trap mass spectrometer or an Agilent 6130 single quadrupole mass spectrometer. High resolution spectra were acquired using a 9.4 T IonSpec QFT-MS FT-ICR mass spectrometer. MS (MALDI-TOF) spectra were performed on a BRUKER REFLEX III instrument that was equipped with a nitrogen laser operating at 337 nm and recorded in the positive-polarity mode. Electrochemical measurements were performed on an Autolab PGStat 30 equipment using a three electrode configuration system. The measurements were carried out using dry CH₂Cl₂ solutions containing 0.1 M tetrabutylammonium hexafluorophosphate (TBAPF₆) and a concentration of approximately 10⁻⁴ M of the corresponding compound. A glassy carbon electrode (3 mm diameter) was used as the working electrode, and a platinum wire and an Ag/AgNO₃ (in CH₃CN) electrode were employed as the counter and the reference electrodes, respectively. Ferrocene (Fc) was used as an internal reference and all the potentials were given relative to the Fc/Fc⁺ couple. Scan rate was 100 mV s⁻¹ unless otherwise specified.

4-(bis(2',4'-bis(hexyloxy)-[1,1'-biphenyl]-4-yl) amino) benzaldehyde (**3**),¹ F₁₂SubPc **7**,² and ZnPc **6**³ were prepared according to literature procedures.

2. Synthetic procedures

5,10,15–Tris(bis(2',4'-bis(hexyloxy)-[1,1'-biphenyl]-4-yl)amino)phenyl–20–(trimethylsilyl) porphyrin (4)

A mixture of **3** (1.34 g, 1.58 mmol), 3-(trimethylsilyl)-2-propynal (0.78 μ L, 0.53 mmol) freshly distilled pirrol (0.15 mL, 2.11 mmol), BF₃OEt₂ (88 μ L, 0.71 mmol), EtOH (1.5 mL) in 211 ml of CHCl₃ was stirred at r.t. for two hours. After that, DDQ (360 g, 1.59 mmol) was added, and the mixture was left stirring at r.t. for one further hour. Finally, addition of Et₃N (0.35 mL) and filtration through silica gave a crude mixture, which was purified by column chromatography on silica gel (heptane/toluene 1:3) and washed with MeOH to give the desired product. Yield: 114 mg, 8%.

¹H-NMR (300 MHz, CHCl₃), δ (ppm): 9.61 (d, J = 4.8 Hz, 2H), 9.00 (d, J = 4.8 Hz, 2H), 8.91 (s, 4H), 8.01 (m, 6H), 7.57 – 7.45 (m, 18H), 7.39 (m, 12H), 7.26 (m, 6H), 6.50 (m, 12H), 3.93 (t, J = 6.5 Hz, 24H), 1.81 – 1.65 (m, 24H), 1.43 – 1.37 (m, 24H), 1.32 – 1.24 (m, 48H), 0.91 – 0.72 (m, 36H), 0.56 (s, 9H), -2.34 (s, 2H).

¹³C-NMR (75 MHz, CHCl₃), δ (ppm): 159.77, 157.23, 147.90, 146.10, 135.72, 135.63, 135.32, 133.63, 131.08, 130.60, 124.44, 123.29, 121.45, 121.27, 105.57, 100.84, 77.16, 68.64, 68.30, 31.78, 31.63, 29.85, 29.50, 29.28, 25.94, 22.78, 22.75, 14.20, 0.52.

HR-MS (MALDI-TOF) m/z Calcd for [C₁₈₇H₂₂₉N₇O₁₂Si]: 2792.7288; Found: 2792.7348.

UV-Vis (CHCl₃), λ_{\max} (log ϵ): 673 (4.18), 586 (4.50), 538 (4.28), 425 (5.38), 332 (5.17) nm.

5,10,15–Tris(bis(2',4'-bis(hexyloxy)[1,1'-biphenyl]-4-yl)amino)phenyl–20–(trimethylsilyl) porphyrinato zinc(II) (5)

Zn(OAc)₂ (49 mg, 0.27 mmol) was added to a solution of **4** (70 mg, 0.025 mmol) in CH₂Cl₂ (12 mL) and MeOH (4 mL). The mixture was stirred at r.t. for 30 minutes, after which the solvents were evaporated under vacuo and the residue was extracted with CH₂Cl₂ and washed with MeOH to give compound **5** as a dark green solid. Yield: 69 mg, 96%.

¹H-NMR (300 MHz, CHCl₃), δ (ppm): 9.78 (d, J = 4.7 Hz, 2H), 9.16 (d, J = 4.7 Hz, 2H), 9.08 (m, 4H), 8.16 – 8.01 (m, 6H), 7.68 – 7.52 (m, 18H), 7.46 (m, 12H), 7.34 (m, 6H), 6.58 (m, 12H), 4.01 (t, J = 5.6 Hz, 24H), 1.80 (m, 24H), 1.52 – 1.47 (m, 24H), 1.38 – 1.31 (m, 48H), 0.95 – 0.85 (m, 36H), 0.62 (s, 9H).

HR-MS (MALDI-TOF) m/z Calcd for [C₁₈₇H₂₂₇N₇O₁₂SiZn]: 2854.6423; Found: 2854.6451.

UV-Vis (THF), λ_{\max} (log ϵ): 622 (4.43), 576 (4.27), 441 (5.31), 327 (5.12) nm.

1,4,15,18-Tetrakis (3,5-bis(trifluoromethyl)phenyl)-9-(ethynyl-3'-phenol)–23[24]-iodo zinc(II) phthalocyanine (10)

To a solution of **6** (0.06 mmol, 100 mg) in freshly distilled THF (3.5 mL) were added Et₃N (1.5 mL), Pd(PPh₃)₄ (10% mol, 7 mg) and CuI (10% mol, 1.1 mg). The mixture was deoxygenated by bubbling argon through it for 20 min. 3-ethynylphenol (0.06 mmol, 6 μ L) was subsequently added and the mixture was stirred at 58°C for 40 minutes. Then, solvents were evaporated and the crude mixture was dissolved in CH₂Cl₂ and washed with water. The combined organic layers were dried over MgSO₄ and concentrated in vacuo. Purification by column chromatography on silica gel (heptane / THF 4:1) gives the desired product as a blue solid, which was washed with heptane. Yield: 30 mg, 30%.

¹H-NMR (300 MHz, THF-*d*₈), δ (ppm): 8.88-8.84 (m, 8H), 8.62 (s, 4H), 8.36-8.25 (m, 8H), 8.12-8.07 (m, 1H), 8.00-7.97 (m, 1H), 7.38-7.27 (m, 3H; H-6', H-7', H-8'), 7.22 (s, 1H; H-4').

MS (MALDI-TOF) m/z for $[C_{72}H_{27}F_{24}IN_8OZn] [M]^+$: 1666.0.

UV-Vis (THF), λ_{max} (log ϵ): 699 (5.03), 674 (5.02), 640 (4.42), 614 (4.35), 356 (4.67), 215 (5.02) nm.

(3-Ethynylphenoxy)-F₁₂SubPc (11)

A mixture of 3-ethynylphenol (0.154 mmol, 17 μ L), **7** (0.077 mmol, 50 mg) and DIPEA (0.154 mmol, 27 μ L) in toluene (5 mL) was refluxed for 8 h. upon cooling, the solvent was evaporated under vacuo and the residue was purified by column chromatography on silica gel (heptane/toluene 1:1) to give the desired compound as a purple powder. Yield: 21 mg, 38%.

¹H-NMR (300 MHz, CHCl₃), δ (ppm): 6.83 (dt, $J_1 = 9$ Hz, $J_2 = 1.2$ Hz, 1H), 6.75 (t, $J = 9$ Hz, 1H), 5.56 (s, 1H), 5.28-5.24 (m, 1H), 2.91 (s, 1H).

HR-MS (MALDI-TOF) m/z Calcd for $[C_{32}H_5F_{12}N_6BO]$: 728.0426; Found: 728.0418.

ZnPc-F₁₂SubPc (8)

In a 25-mL round-bottomed flask, equipped with a magnetic stirrer, **7** (0.017 mmol, 11 mg) and AgOTf (0.02 mmol, 6 mg) were placed. Dry toluene (1.5 mL) was added and the mixture was stirred at 60°C under argon atmosphere until the **7** is consumed (easily monitored by TLC heptane/THF 3:1). Once the intermediate triflate-F₁₂SubPc is generated, a solution of **10** (0.017 mmol, 26 mg) and freshly distilled DIPEA (0.023 mmol, 3 μ L) in dry toluene (2 mL) was added. The mixture was stirred at reflux for 5 hours. The solvent was removed by evaporation under reduced pressure and the product was directly purified by chromatography on silica gel using toluene as eluent. The second fraction of the column is the desired compound, which was washed with MeOH/H₂O (10:1) to afford **8** as a dark violet solid. Yield: 6 mg, 15%.

¹H-NMR (300 MHz, THF-*d*₈), δ (ppm): 8.85 (m, 6H), 8.80 (s, 2H), 8.59 (s, 4H), 8.137 (s, 1H), 8.31-8.25 (m, 6H), 8.21-8.17 (m, 1H), 7.97-7.93 (m, 2H), 7.14 (d, $J = 7,8$ Hz, 1H), 7.00 (t, $J = 7.8$ Hz, 1H), 5.99 (s, 1H), 5.53 (d, $J = 8.7$ Hz, 1H).

MS (MALDI-TOF) m/z Calcd for $[C_{96}H_{26}F_{36}IN_{14}BOZn] [M]^+$: 2276.0; Found: 2276.0

UV-Vis (THF), λ_{max} (log ϵ): 696 (5.02), 675 (5.05), 640 (4.41), 615 (4.38), 567 (4.81), 512 (4.28) 353 (4.70) nm.

BBPA₃ZnPor-ZnPc (9)

TBAF (0.036 mmol, 36 μ L of a 1M solution in THF) was added to a solution of **5** (0.009 mmol, 26 mg) in THF (5 mL) at 0°C and under argon. The reaction mixture was stirred at r.t. for 45 minutes. Once the deprotected BBPA₃Por **2** is generated, and the starting **5** totally consumed (easily monitored by TLC heptane/toluene 1:2), the reaction mixture was poured into water and extract several times with CH₂Cl₂ and dried with MgSO₄. Then, the solvent was evaporated and **2** was used for the next reaction without any further purification. To a solution of **10** (0.009 mmol, 15 mg) in freshly distilled THF (3 mL) were added Et₃N (1.5 mL), Pd₂(dba)₃ (20% mol, 1.6 mg), AsPh₃ (0.009 mmol, 3 mg) and the recently deprotected BBPA₃Por **2** (0.009 mmol). The mixture was deoxygenated by bubbling argon through it for 20 min. The mixture was stirred at 50°C for 20 h. Then, solvents were evaporated and the crude mixture was dissolved in CH₂Cl₂ and washed with water. The combined organic layers were dried over MgSO₄ and concentrated in vacuo. Purification by column chromatography on silica gel

(heptane / THF 3:1) gives the desired product as a dark green solid, which was washed with acetonitrile. Yield: 32 mg, 82%.

¹H-NMR (300 MHz, THF-*d*₈), δ (ppm): 10.13 (d, J = 4.5 Hz, 2H), 9.38 (d, J = 4.5 Hz, 2H), 9.08 (s, 6H), 8.98-8.95 (m, 4H), 8.87 (s, 4H), 8.74 (s, 2H), 8.66 (s, 1H), 8.63 (s, 2H), 8.33-8.28 (m, 6H), 8.24 (d, J = 8.6 Hz, 4H), 8.16 (d, J = 8.3 Hz, 2H), 8.10 (d, J = 7.8 Hz, 1H), 7.70 – 7.57 (m, 20H), 7.54-7.46 (m, 12H), 7.37-7.30 (m, 10H), 6.67 – 6.56 (m, 12H), 4.03 (q, J = 6.3 Hz, 24H), 2.47 (m, 12H), 1.87 – 1.77 (m, 24H), 1.53 (m, 24H), 0.92 (dt, J = 14.1, 5.7 Hz, 36H).

HR-MS (MALDI-TOF) m/z Calcd for [C₂₅₆H₂₄₅F₂₄N₁₅O₁₃Zn₂]: 4322.7210; Found: 4322.7315.

UV-Vis (THF), λ_{max} (log ε): 708 (5.00), 642 (4.52), 581 (4.06), 448 (5.06), 330 (5.01), 256 (4.90) nm.

BBPA₃ZnPor-ZnPc-F₁₂SubPc (1)

In a 25-mL round-bottomed flask, equipped with a magnetic stirrer, **7** (0.035 mmol, 23 mg) and AgOTf (0.0455 mmol, 12 mg) were placed. Dry toluene (2 mL) was added and the mixture was stirred at 50°C under argon atmosphere until the **7** is consumed (easily monitored by TLC heptane/THF 3:1). Once the intermediate triflate-F₁₂SubPc is generated, a solution of **9** (0.007 mmol, 32 mg) and freshly distilled DIPEA (0.0455 mmol, 8 μL) in dry toluene (2 mL) was added. The mixture was stirred at 100°C for 12 hours. The solvent was removed by evaporation under reduced pressure and the product was directly purified by chromatography on silica gel using toluene as eluent. Then the solvent was evaporated under vacuo to afford the desired triad as a dark brown solid. Yield: 2 mg, 6%.

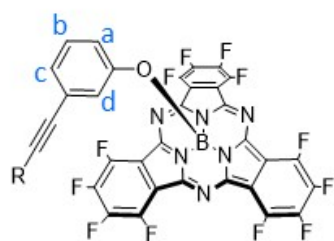
¹H-NMR (300 MHz, THF-*d*₈), δ (ppm): 10.11 (d, J = 4.5 Hz, 2H), 9.37 (d, J = 4.5 Hz, 2H), 9.06 (s, 6H), 8.95 (m, 4H), 8.87-8.80 (m, 4H), 8.72 (s, 2H), 8.61 (s, 2H), 8.39 (s, 2H), 8.32 (m, 4H), 8.23 (d, J = 8.3 Hz, 6H), 8.14 (d, J = 8.6 Hz, 3H), 8.03 – 7.95 (m, 3H), 7.66-7.56 (m, 20H), 7.52-7.44 (m, 12H), 7.40 – 7.26 (m, 10H), 7.16 (d, J = 7.2 Hz, 1H), 7.03 (m, 1H), 6.64 – 6.58 (m, 12H), 6.01 (s, 1H), 5.56 – 5.52 (m, 1H), 4.02 (m, 24H), 1.51 (m, 24H), 1.45 – 1.32 (m, 72H), 0.91 (m, 36H).

HR-MS (MALDI-TOF) m/z Calcd for [C₂₈₀H₂₄₄BF₃₆N₂₁O₁₃Zn₂]: 4931.7222; Found: 4931.7156.

UV-Vis (THF), λ_{max} (log ε): 705 (5.10), 639 (4.68), 568 (4.95), 447 (5.18), 319 (5.24), 261 (5.22) nm.

3. Characterization

3.1 NMR



11: R = H

8: R = ZnPc

1: R = BBPA₃ZnPc-ZnPc 9

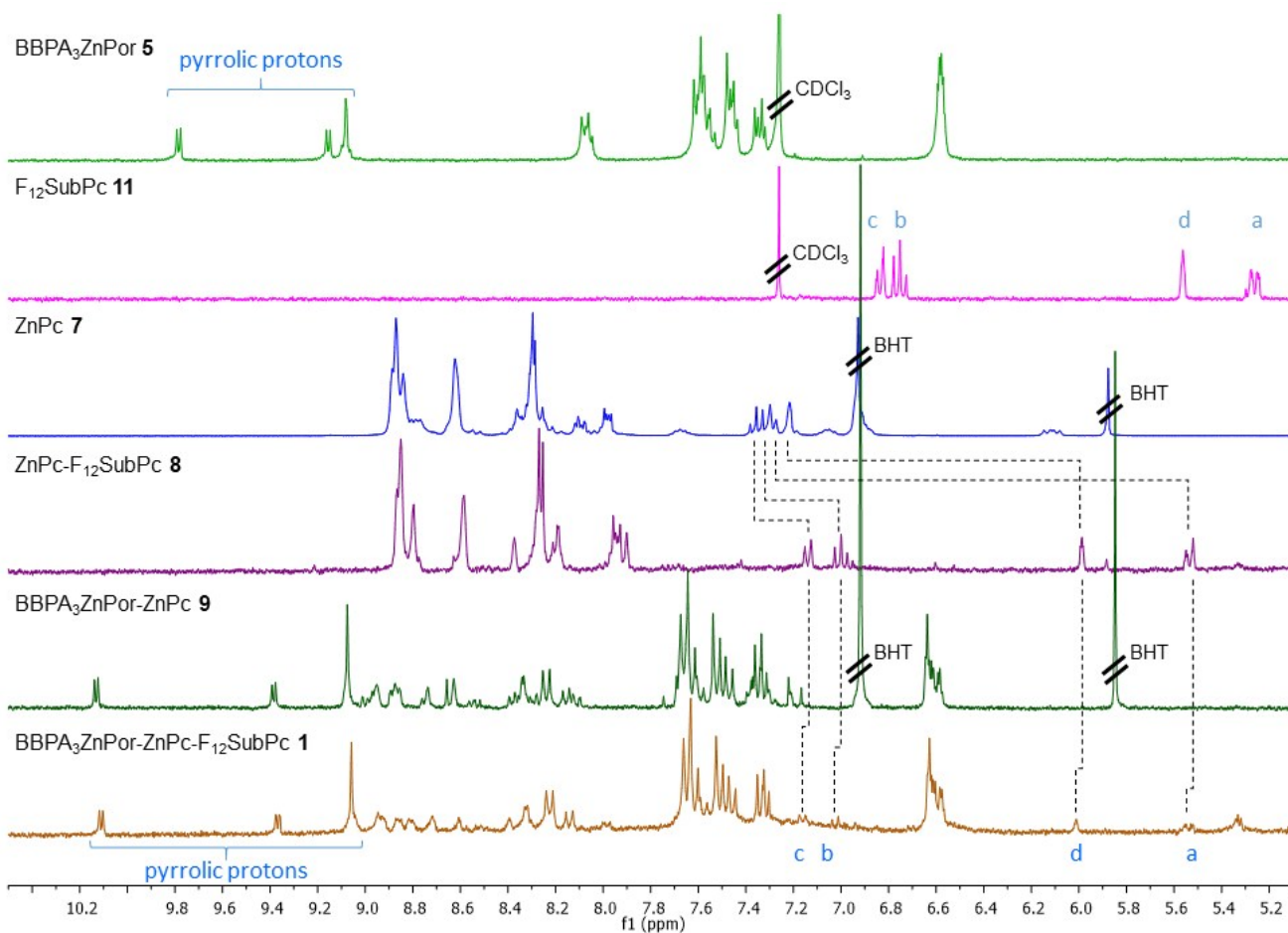


Figure S1. Comparison of ¹H-NMR spectra of **5** and **11** in CDCl₃, and **7**, **8**, **9** and **1** in THF-d₈. Dashed lines are drawn to guide the eye to the changes in chemical shifts of protons Ha, Hb, Hc and Hd.

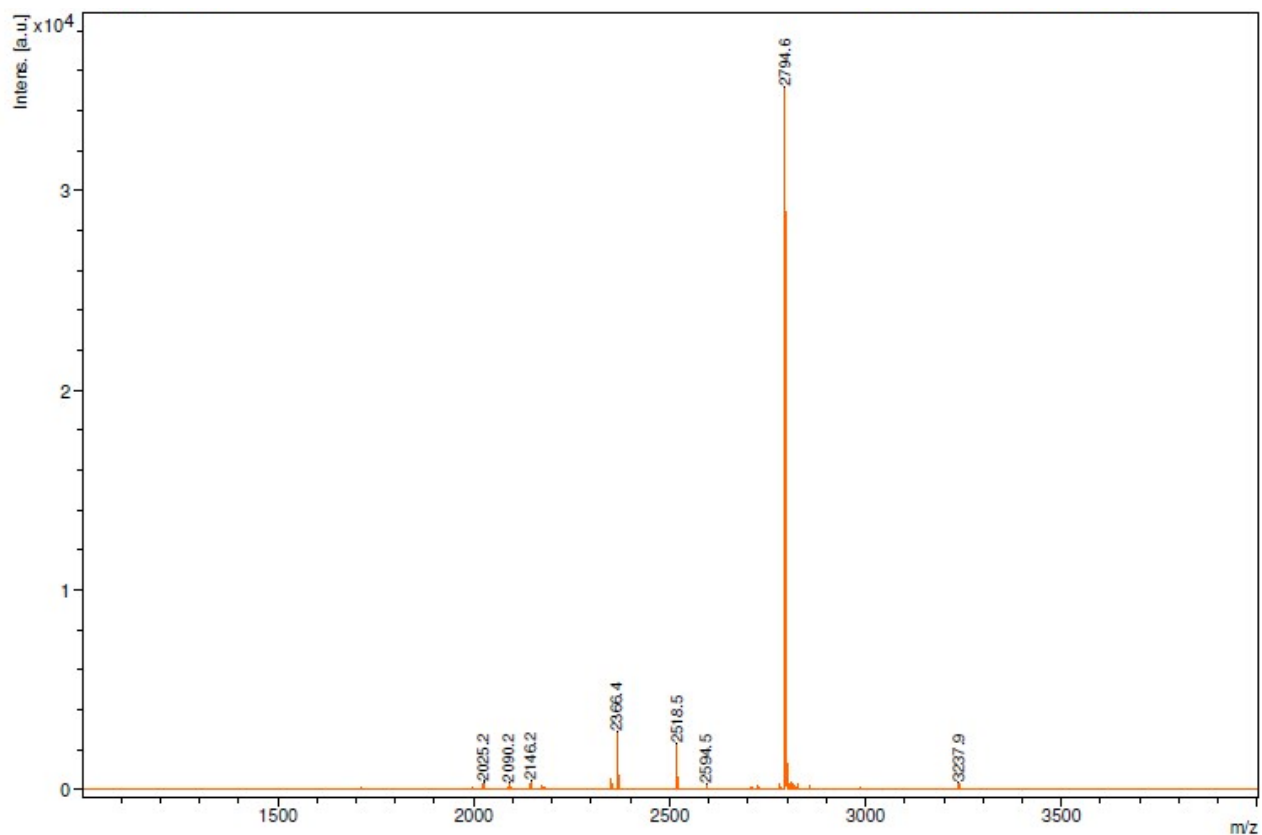


Figure S2: MALDI-TOF mass spectrum of 4.

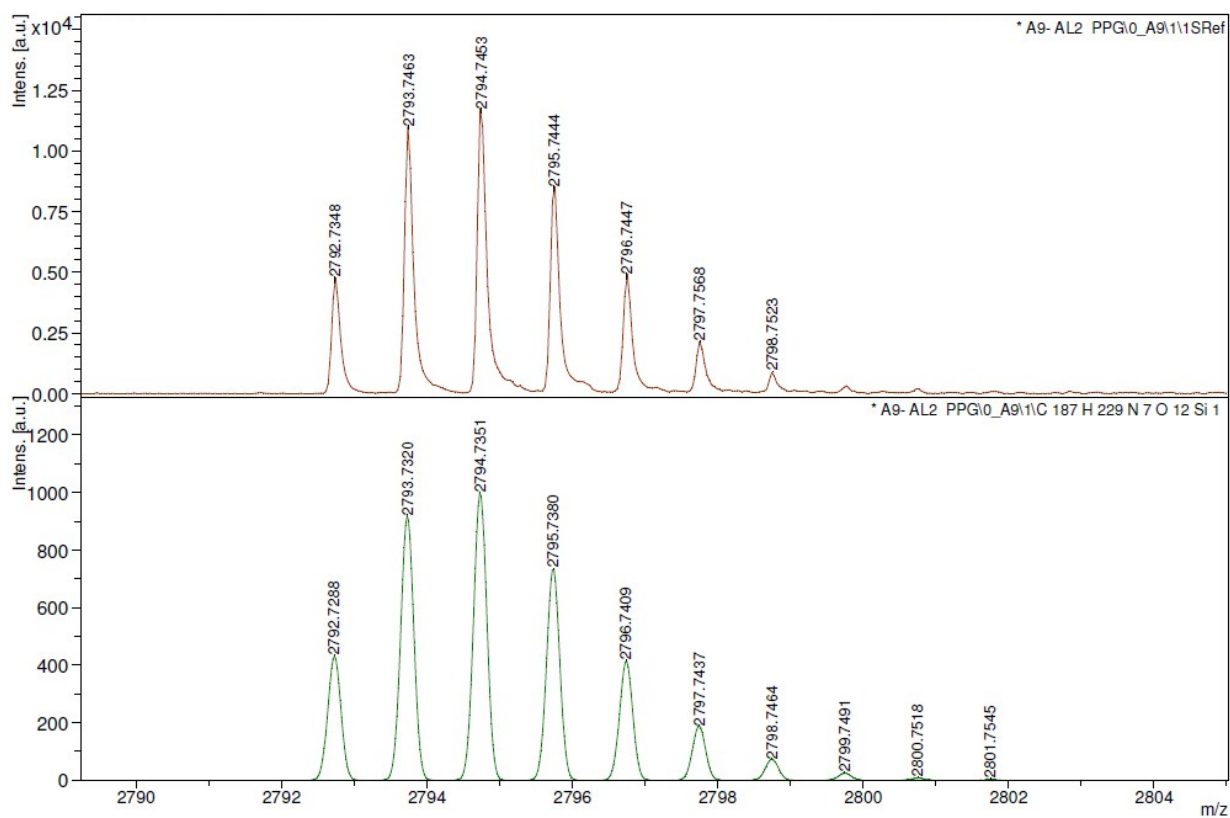


Figure S3. High-resolution MALDI-TOF mass spectrum of 4. Theoretical (bottom) and experimental (top) pattern found for the ion molecular peak $[M]^+$.

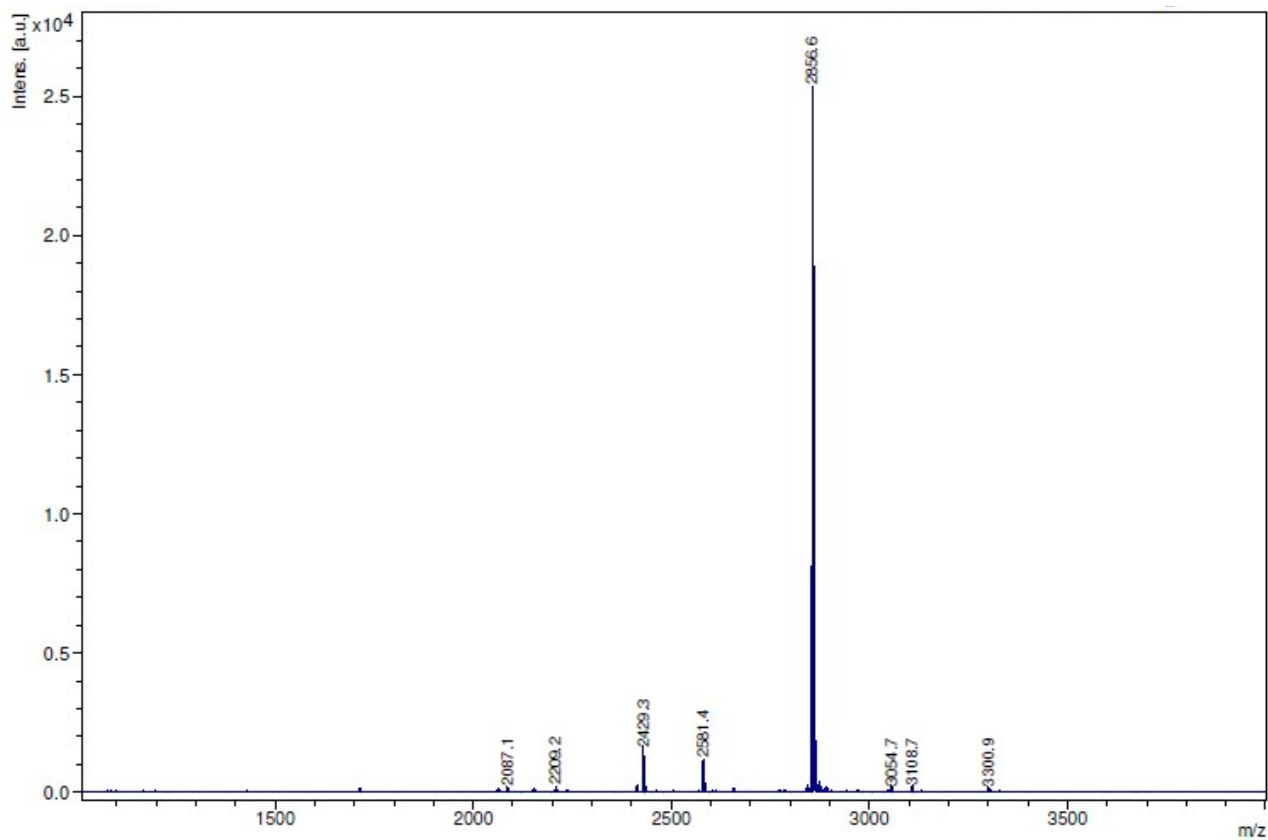


Figure S4: MALDI-TOF mass spectrum of **5**.

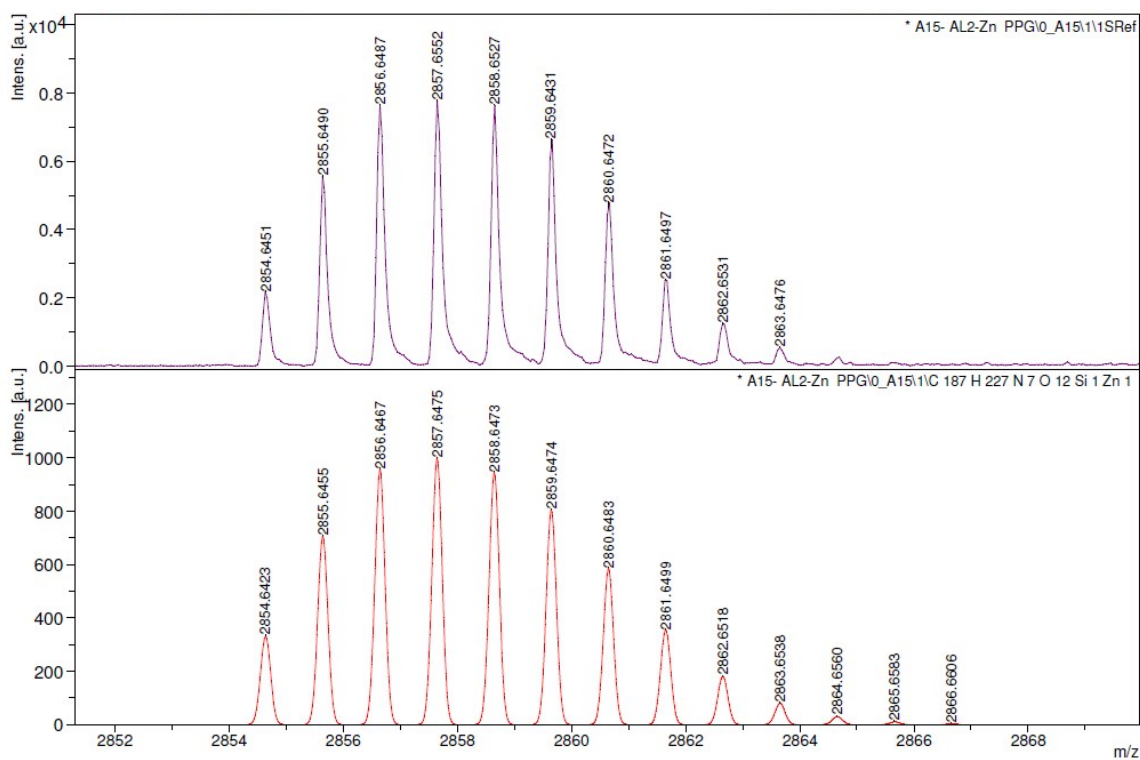


Figure S5. High-resolution MALDI-TOF mass spectrum of **5**. Theoretical (bottom) and experimental (top) pattern found for the ion molecular peak $[M]^+$.

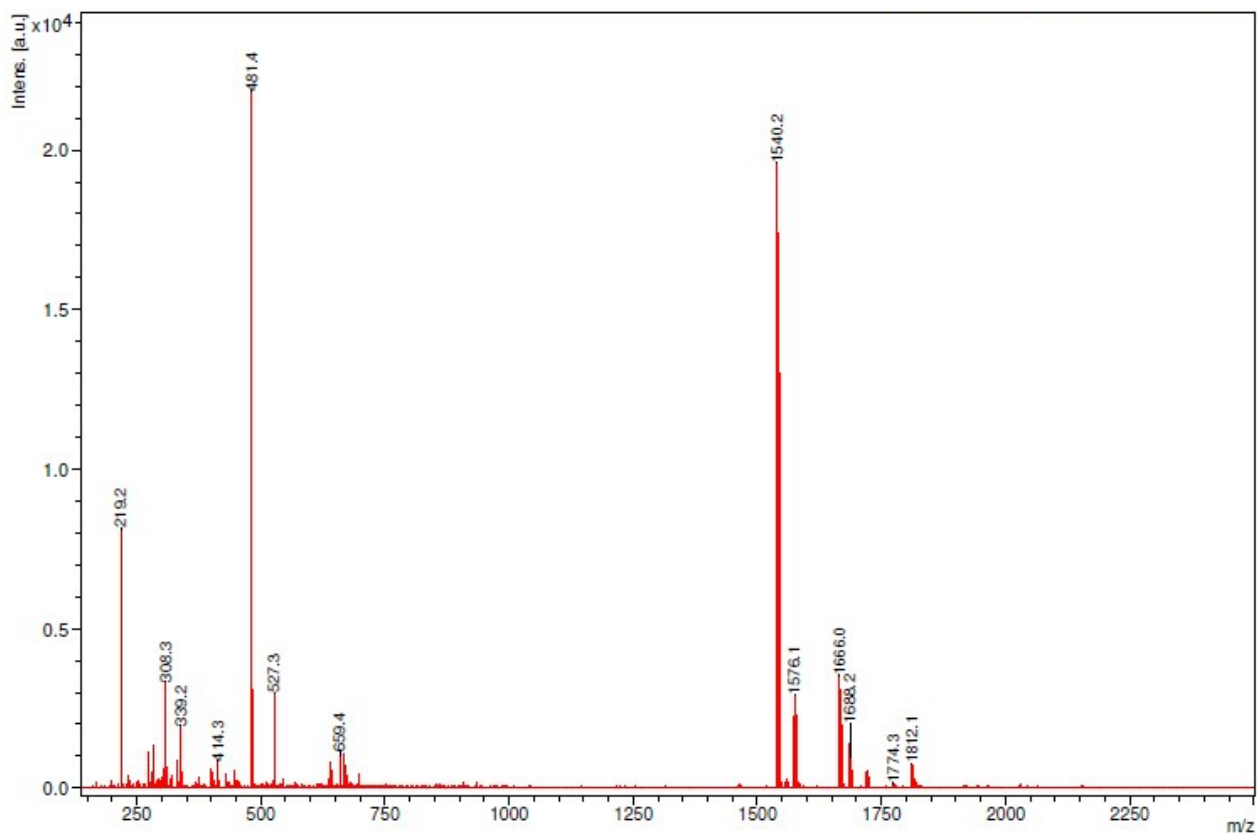


Figure S6: MALDI-TOF mass spectrum of **10**.

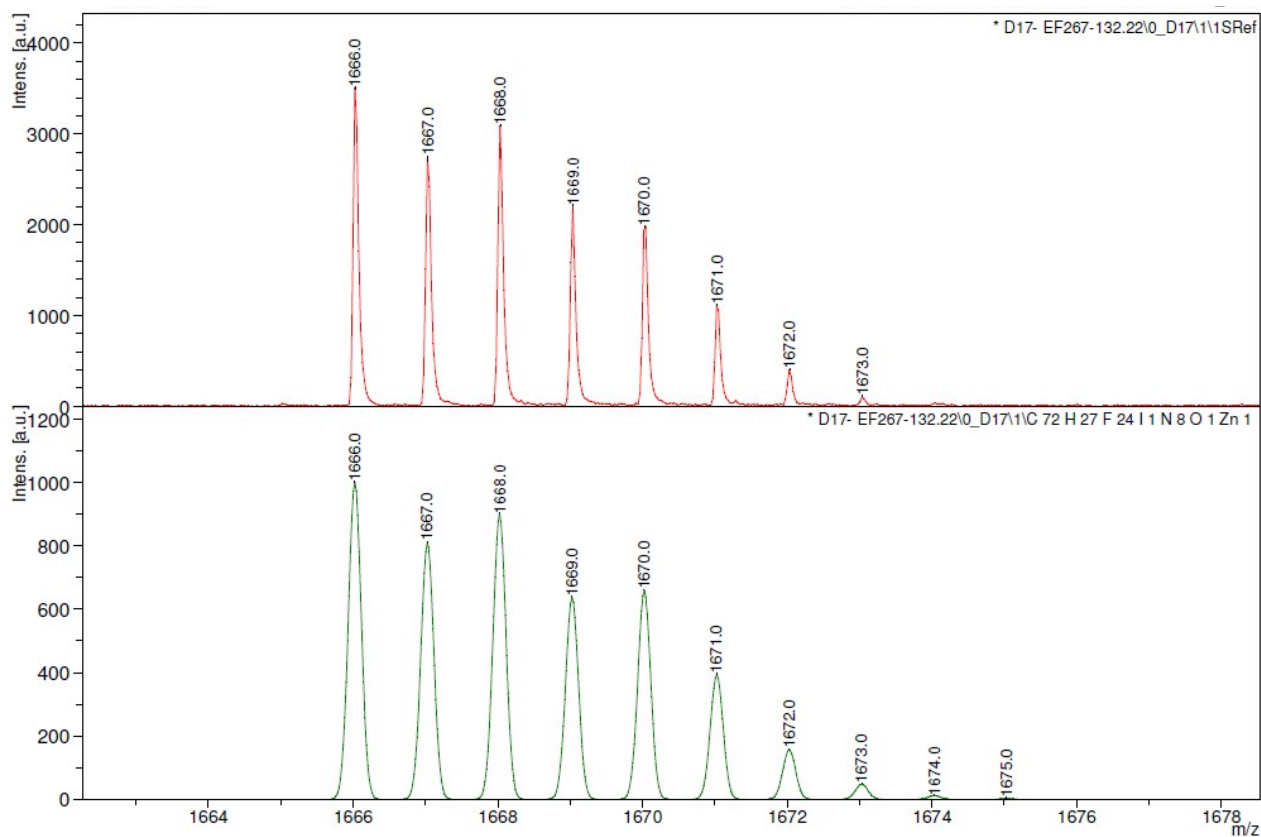


Figure S7. MALDI-TOF mass spectrum of **10**. Theoretical (bottom) and experimental (top) pattern found for the ion molecular peak $[M]^+$.

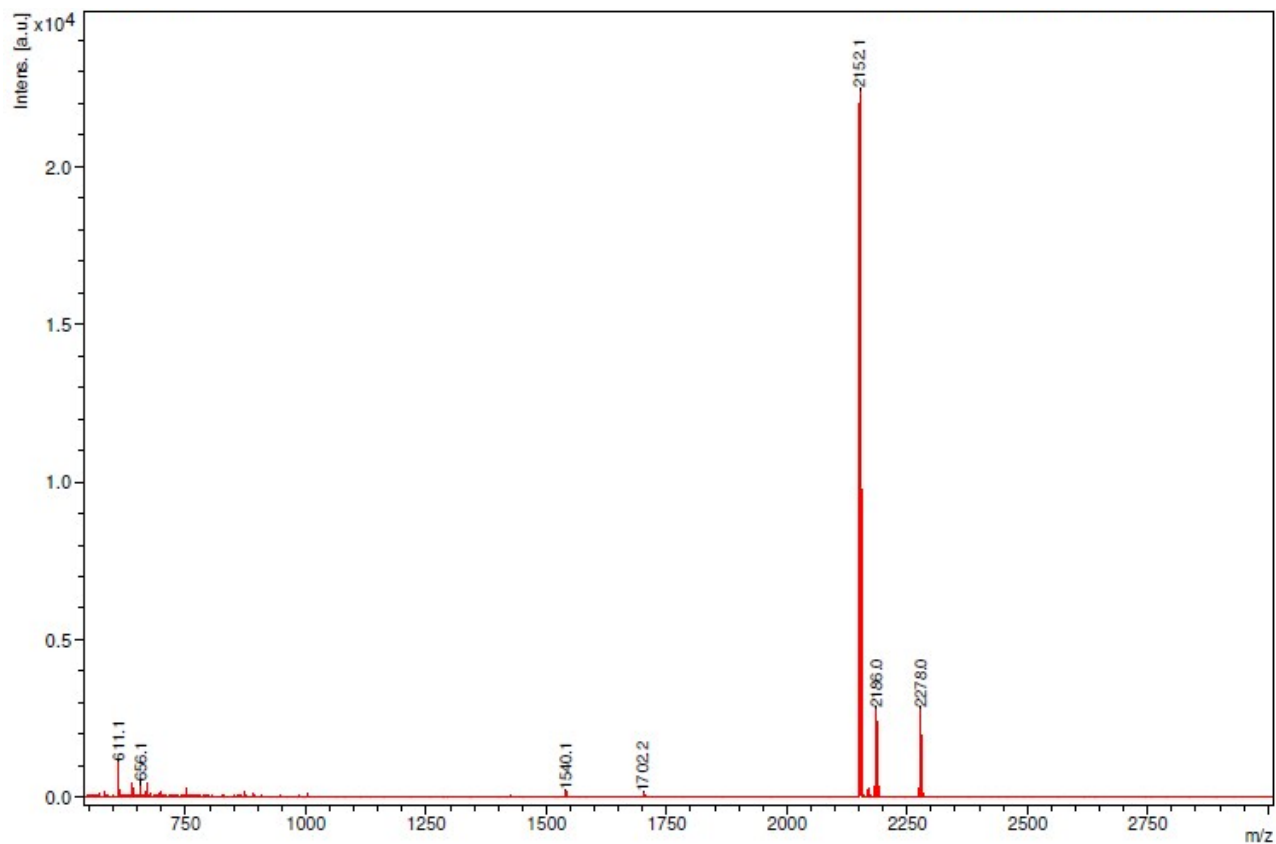


Figure S8: MALDI-TOF mass spectrum of **8**.

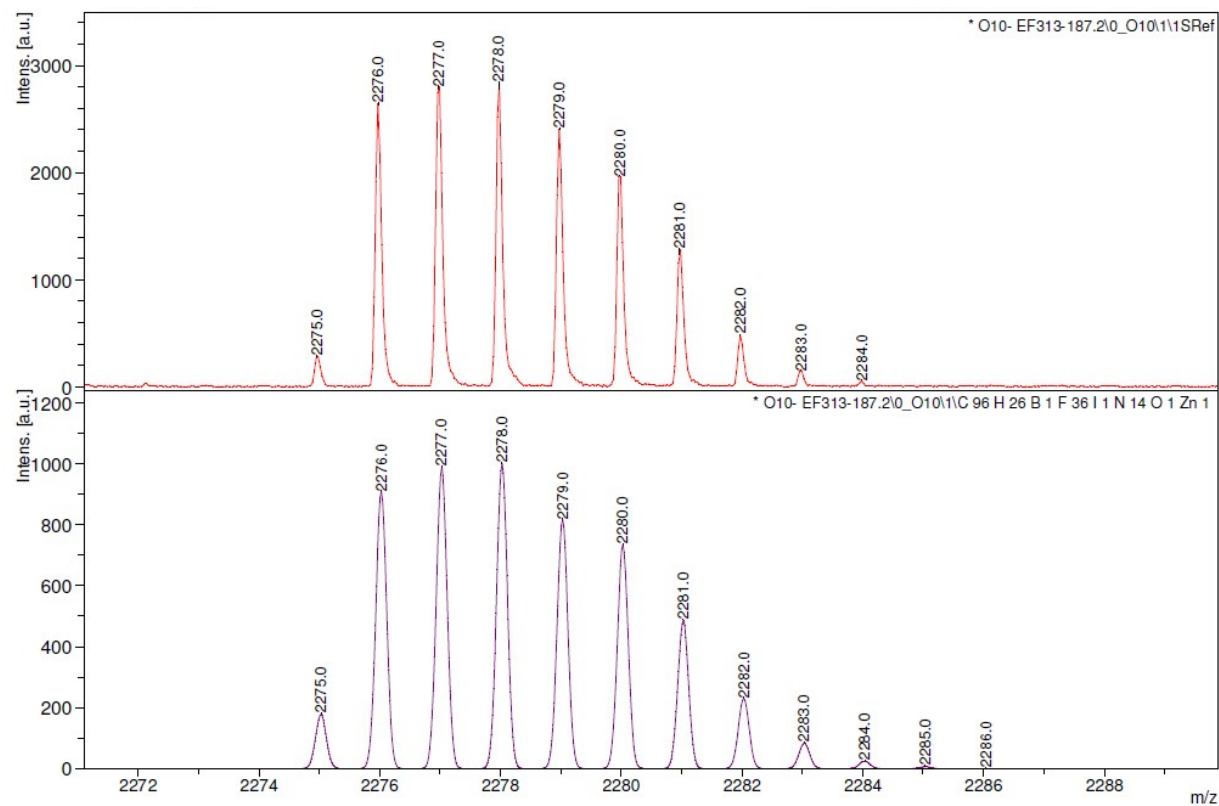


Figure S9. MALDI-TOF mass spectrum of **8**. Theoretical (bottom) and experimental (top) pattern found for the ion molecular peak $[M]^+$.

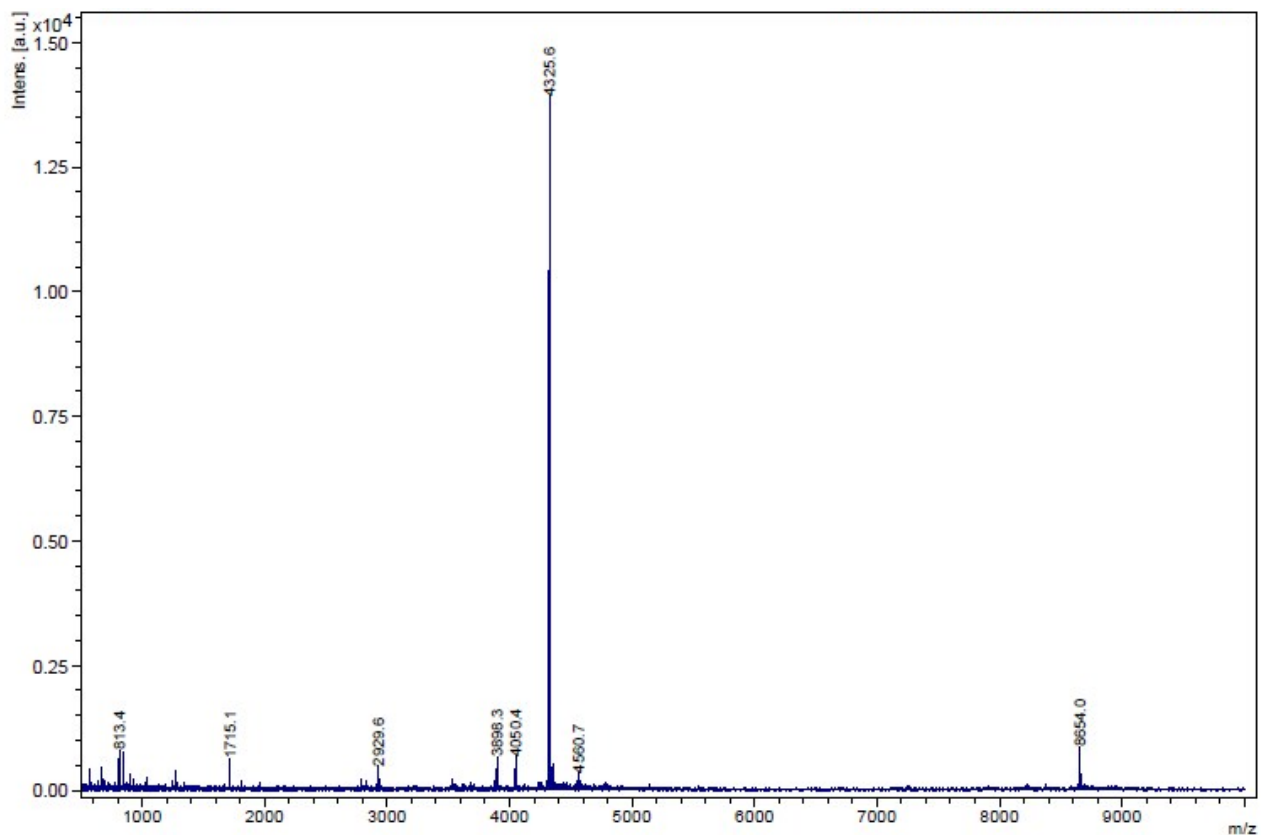


Figure S10: MALDI-TOF mass spectrum of **9**.

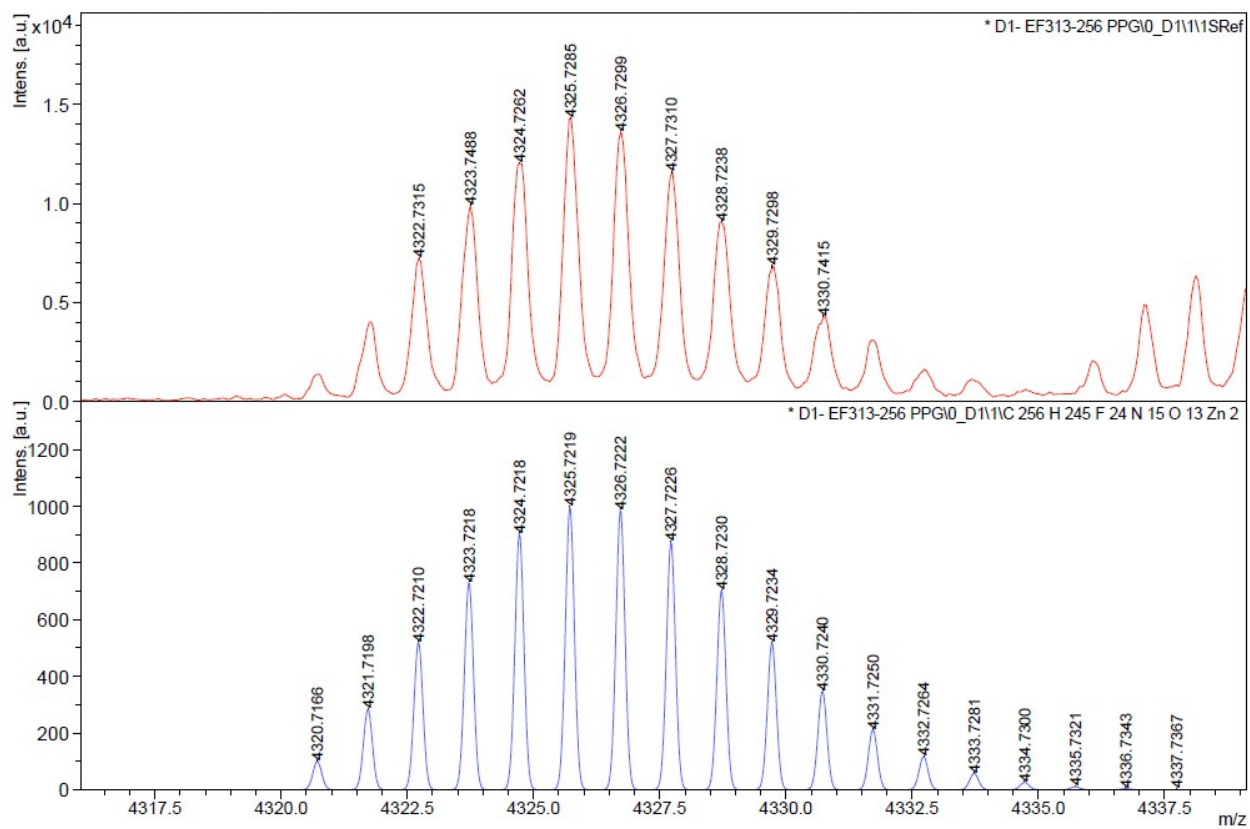


Figure S11. High-resolution MALDI-TOF mass spectrum of **9**. Theoretical (bottom) and experimental (top) pattern found for the ion molecular peak $[M]^+$.

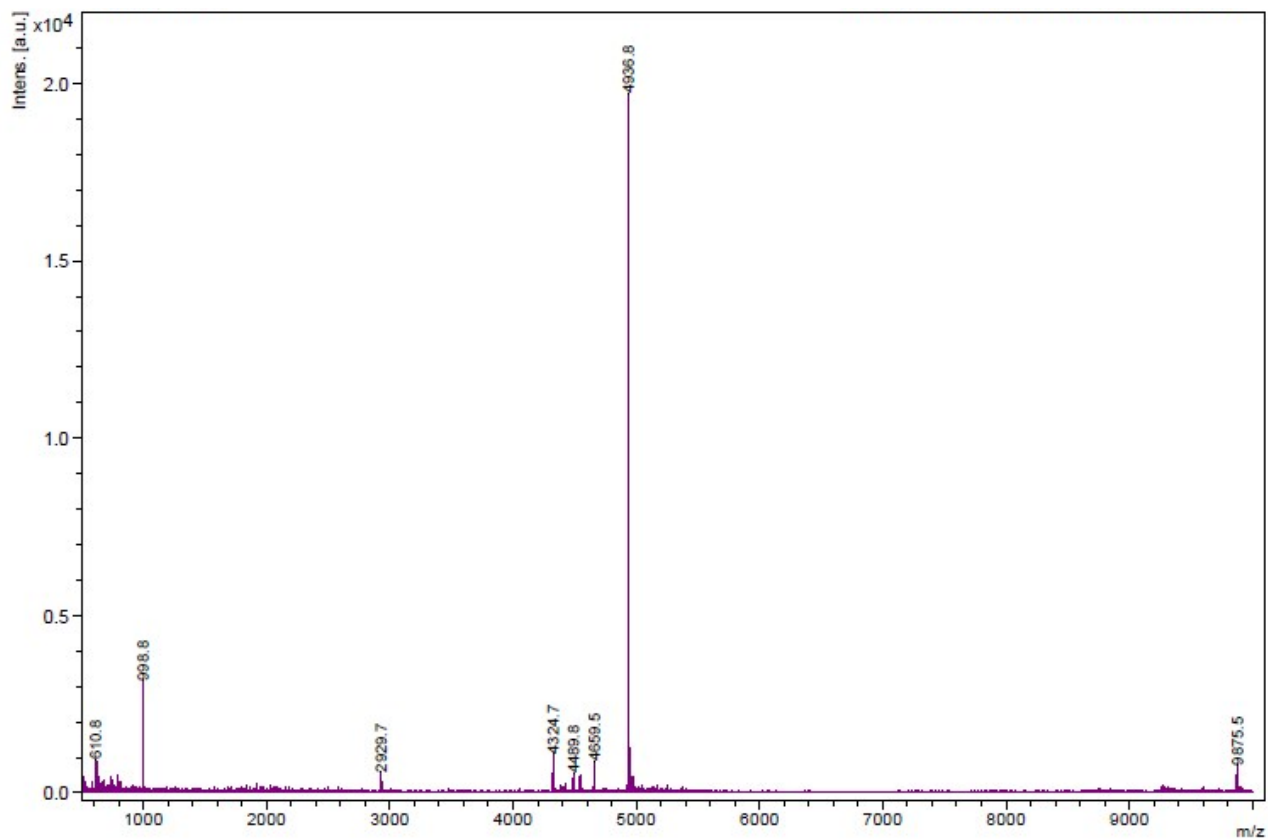


Figure S12: MALDI-TOF mass spectrum of **1**.

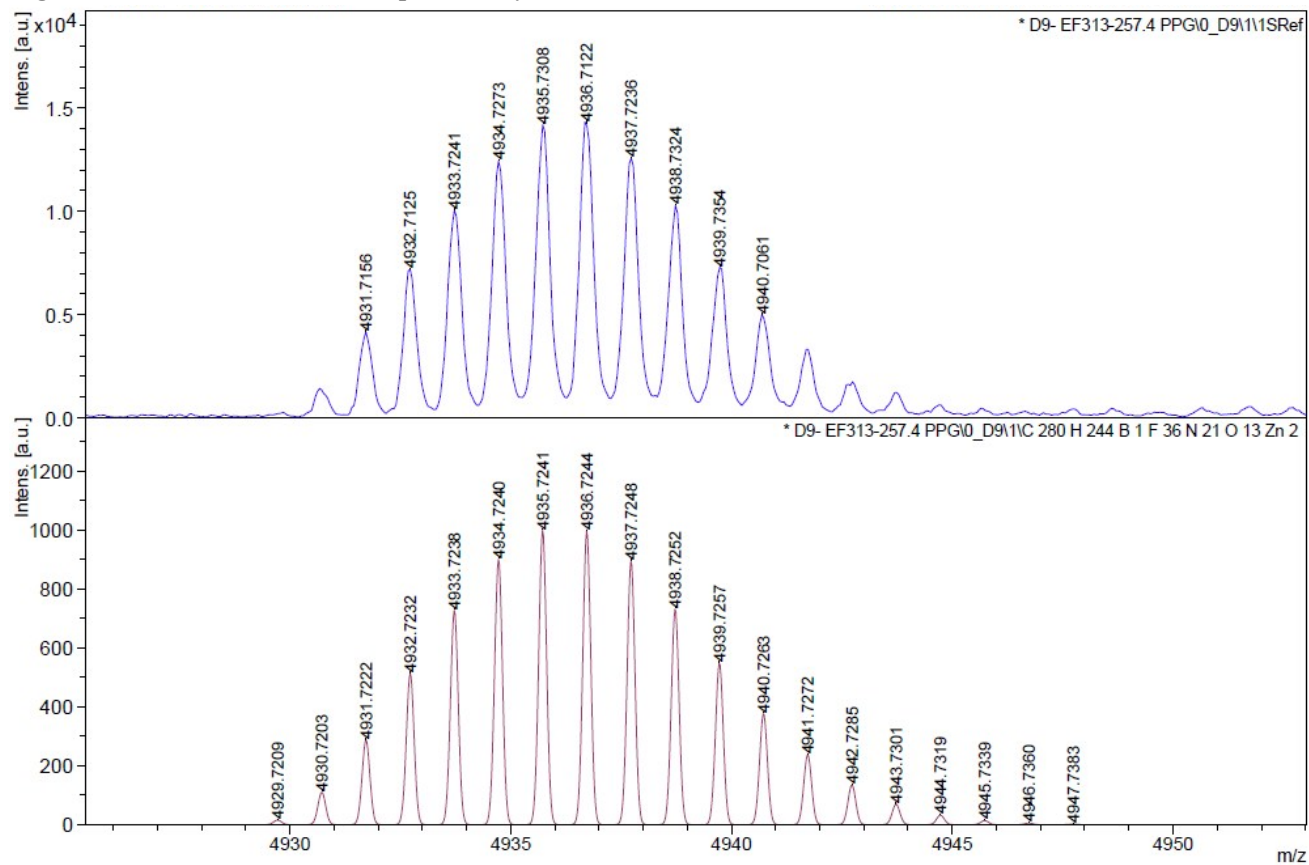


Figure S13. High-resolution MALDI-TOF mass spectrum of **1**. Theoretical (bottom) and experimental (top) pattern found for the ion molecular peak $[M]^+$.

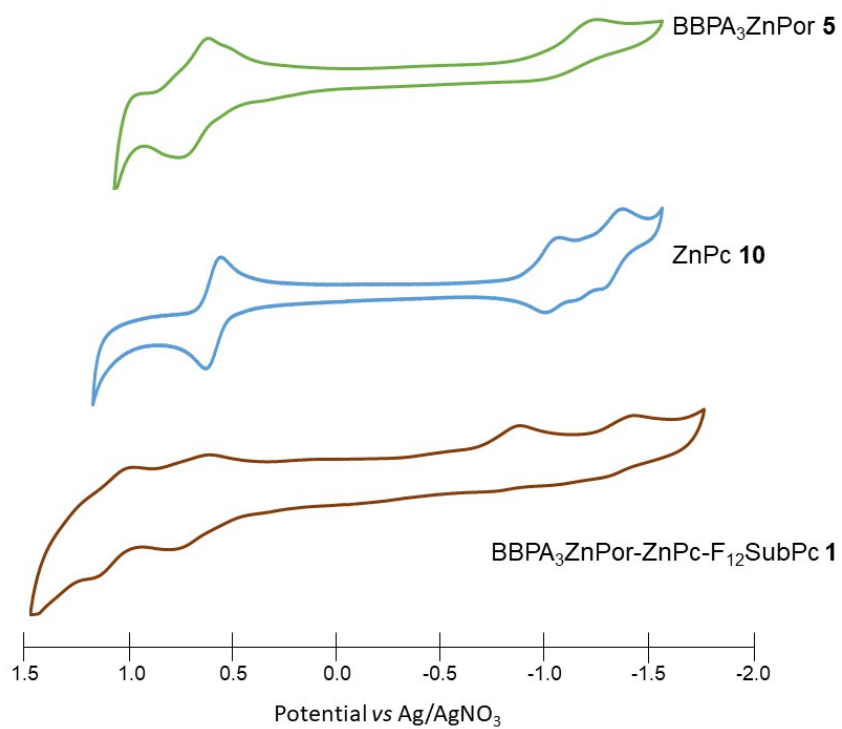


Figure S14. Cyclic voltammograms of **5**, **10** and **1**. Potential values are registered vs Ag/AgNO₃ reference electrode.

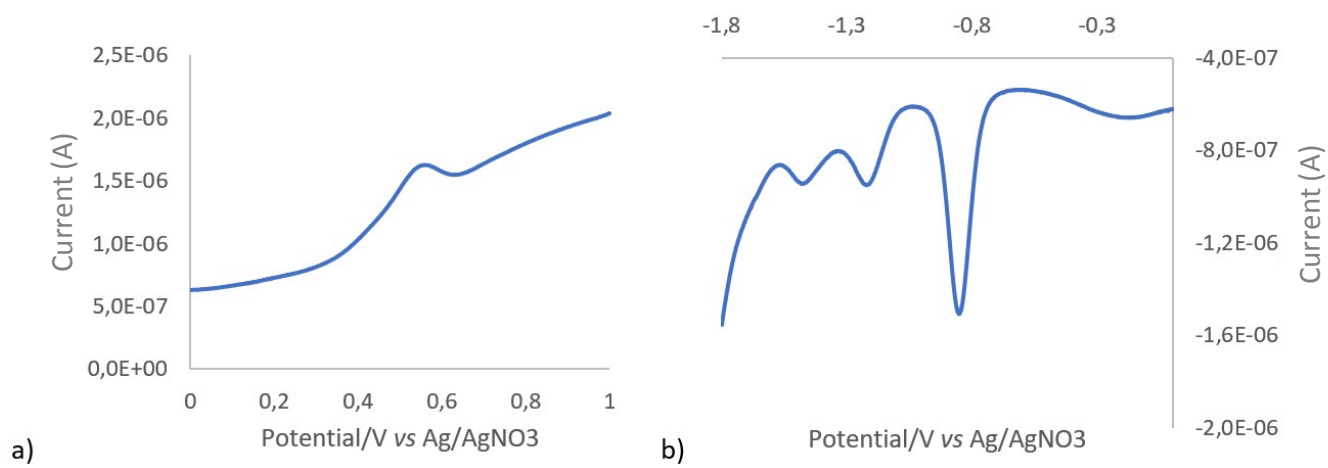
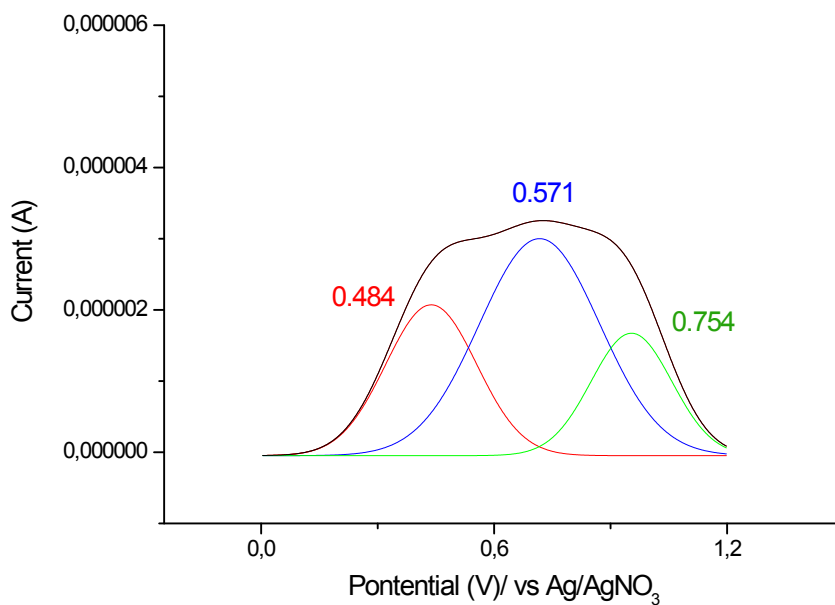
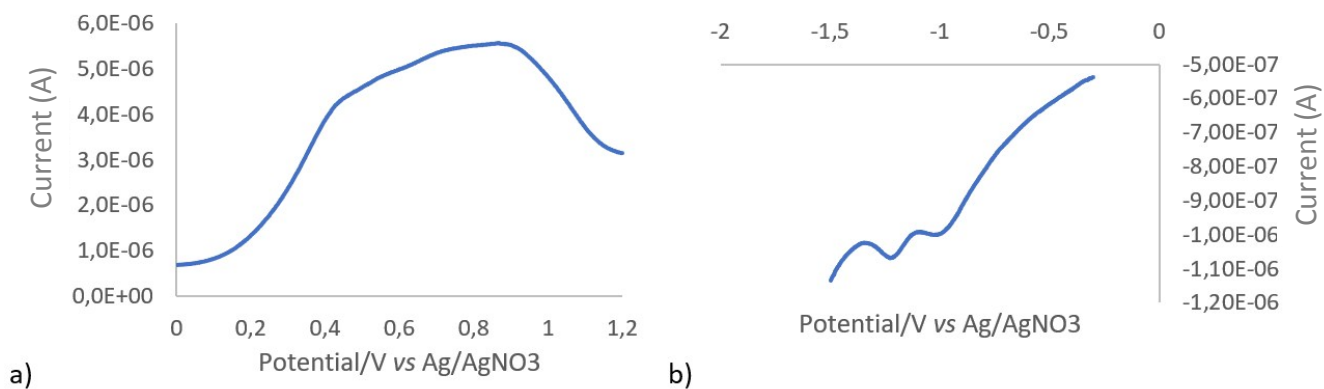


Figure S15. Square-wave voltammograms of **8**: a) oxidation, b) reduction.



c)
Figure S16. Square-wave voltammograms of **9**: a) oxidation, b) reduction, c) deconvolution of the oxidation processes.

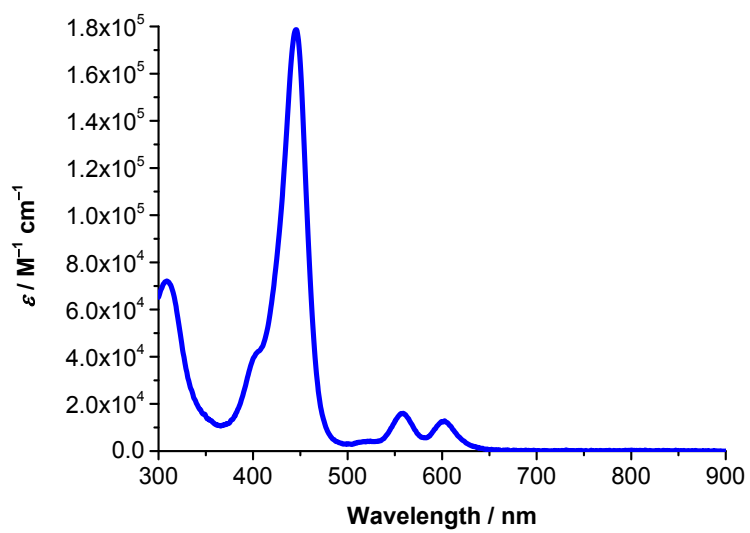


Figure S17. Steady state absorption spectrum of 5 in toluene.

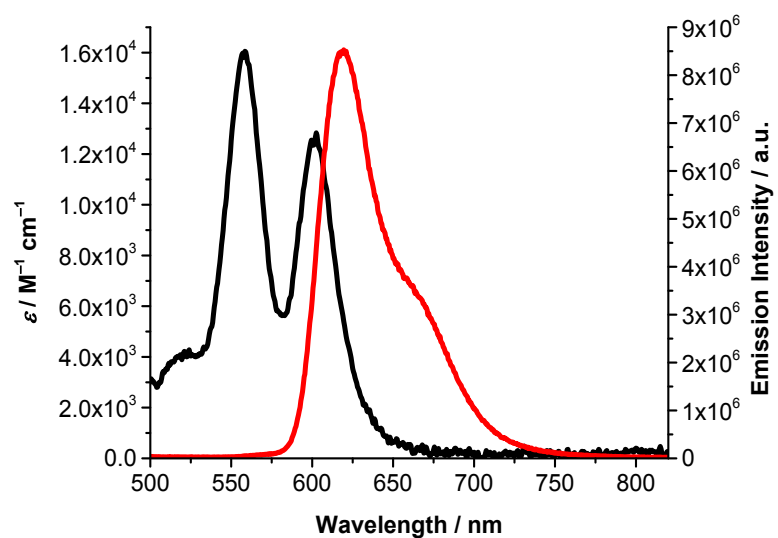


Figure S18. Steady state absorption (black) and fluorescence spectra (red) of **5** ($7.84 \times 10^{-7} \text{ M}$) recorded upon 430 excitation in toluene.

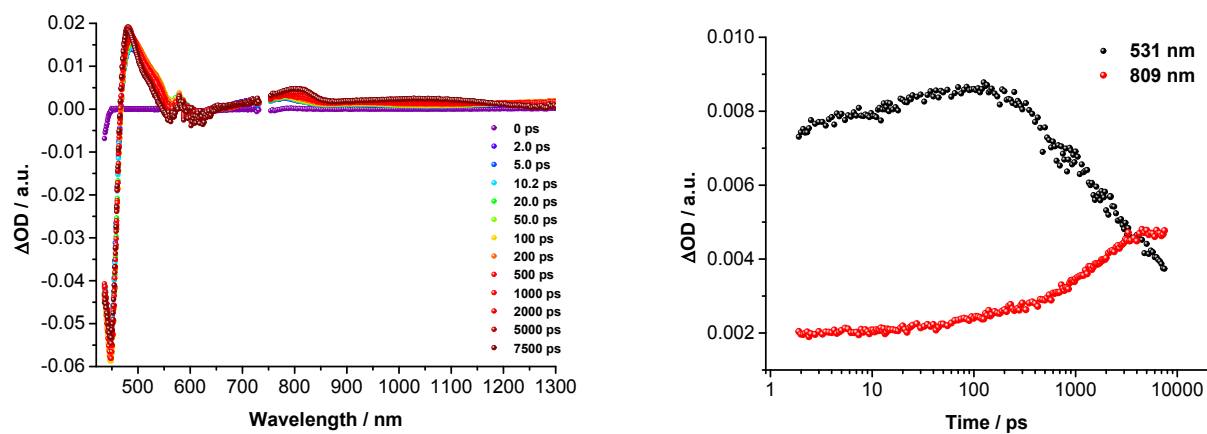


Figure S19. Differential absorption spectra (left) obtained upon femtosecond flash photolysis (430 nm, 500 nJ) of **5** (2.5×10^{-5} M) in argon-saturated toluene with several time delays between 0 and 7500 ps at room temperature; see legend for time evolution. Time absorption profiles (right) at 531 nm (black) and 809 nm (red) illustrating the excited state decay.

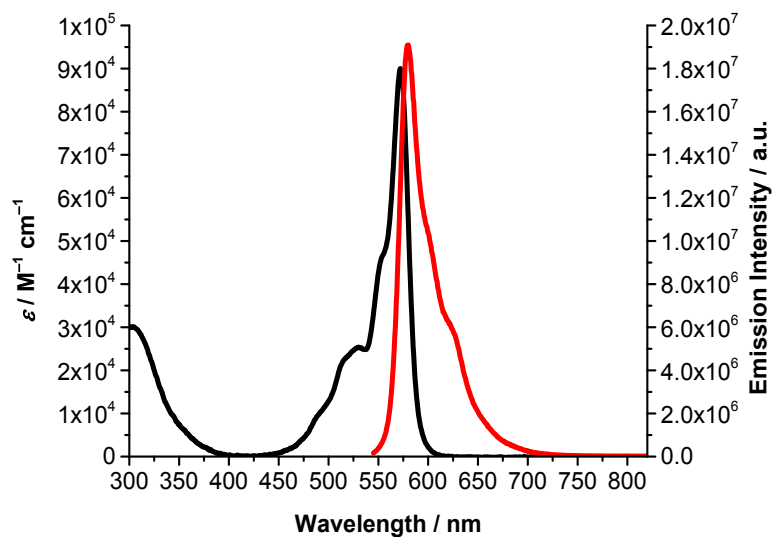


Figure S20. Steady state absorption (black) and fluorescence spectra (red) of **11** ($1.24 \times 10^{-6} \text{ M}$) recorded upon 530 excitation in toluene.

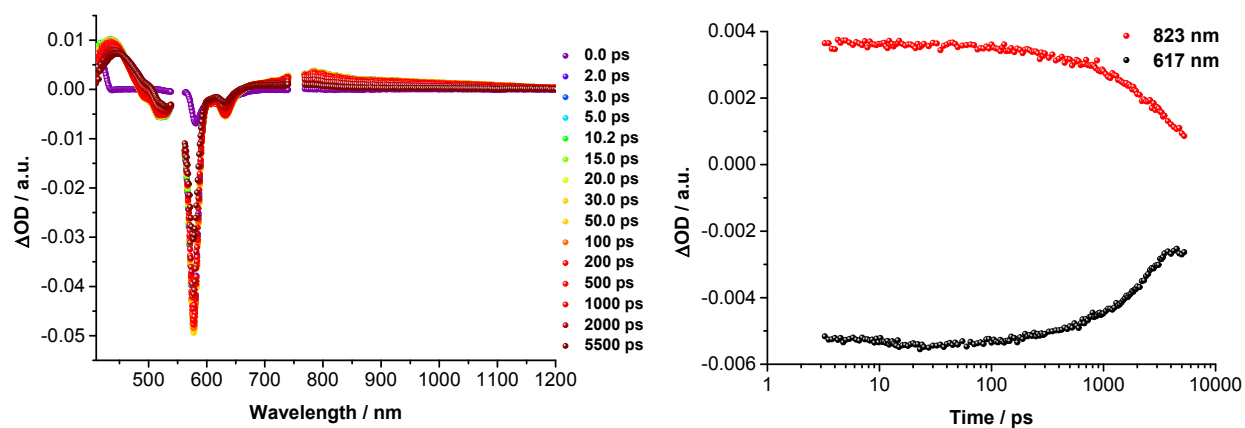


Figure S21. Differential absorption spectra (left) obtained upon femtosecond flash photolysis (550 nm, 150 nJ) of **11** ($2 \times 10^{-5} M$) in argon-saturated toluene with several time delays between 0 and 5500 ps at room temperature; see legend for time evolution. Time absorption profiles (right) at 617 nm (black) and 823 nm (red) illustrating the excited state decay.

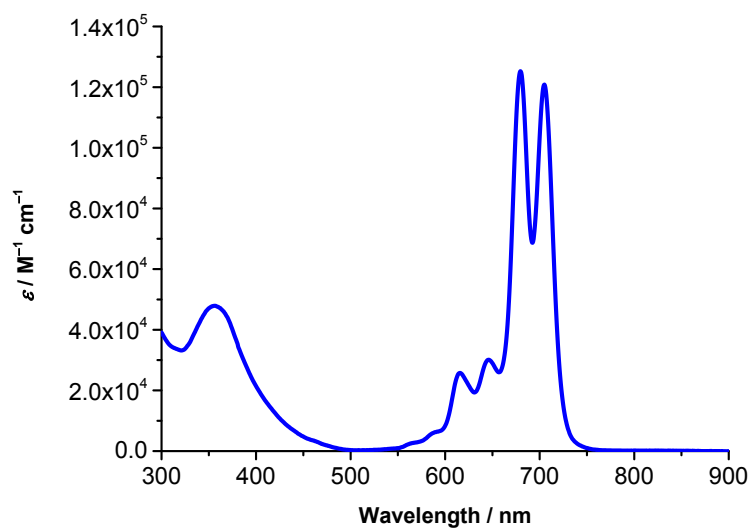


Figure S22. Steady state absorption spectrum of **10** in toluene.

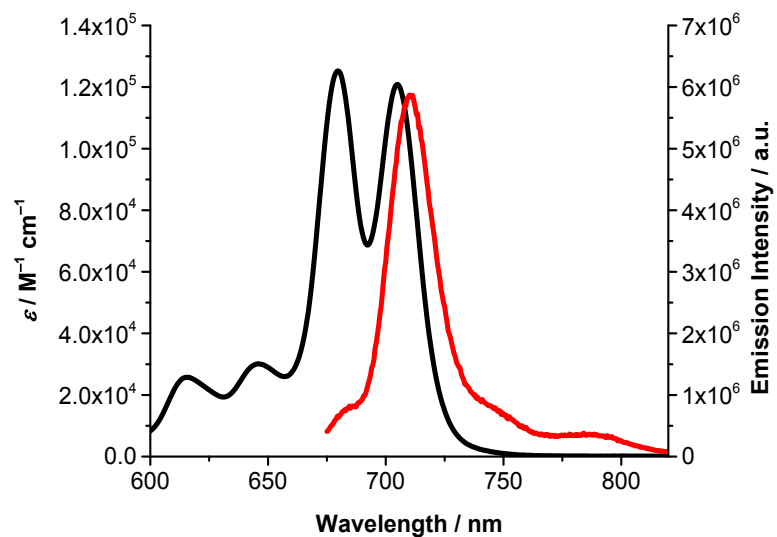


Figure S23. Steady state absorption (black) and fluorescence spectra (red) of **10** ($9.38 \times 10^{-7} \text{ M}$) recorded upon 660 excitation in in toluene.

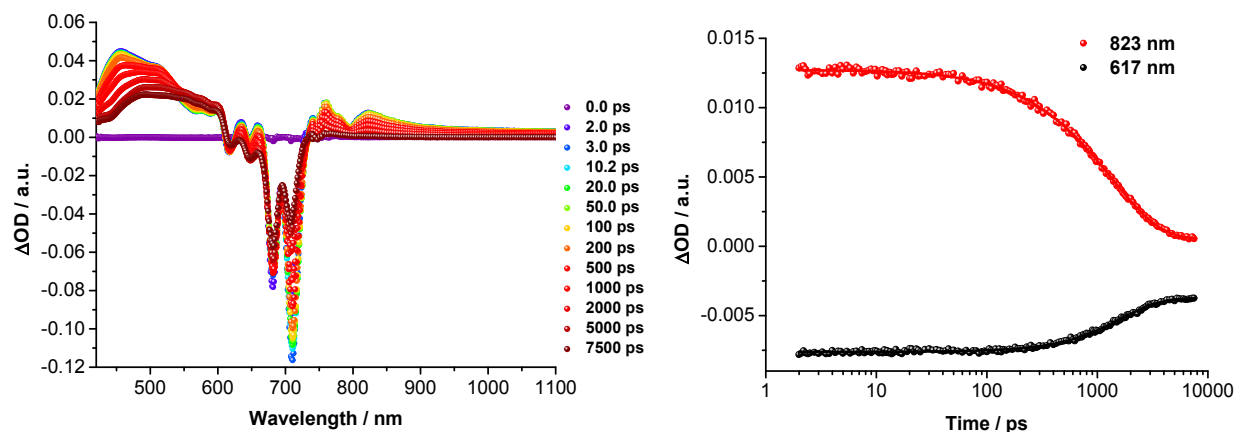


Figure S24. Differential absorption spectra (left) obtained upon femtosecond flash photolysis (676 nm, 200 nJ) of reference 10 (2.5×10^{-5} M) in argon-saturated toluene with several time delays between 0 and 7500 ps at room temperature; see legend for time evolution. Time absorption profiles (right) at 617 nm (black) and 823 nm (red) illustrating the excited state decay.

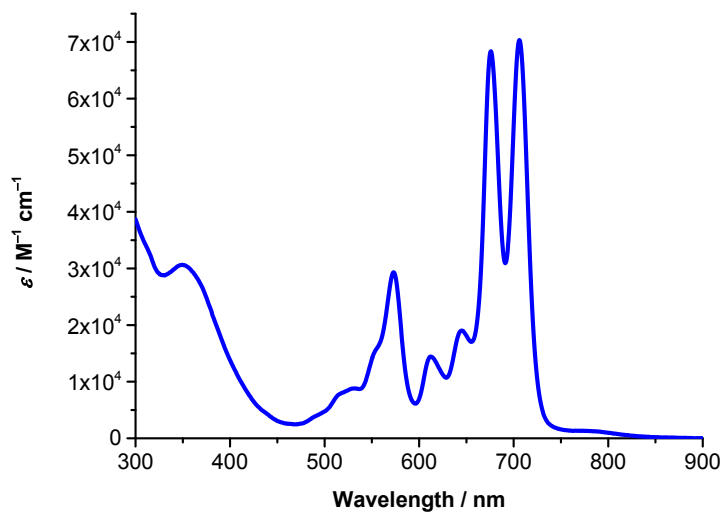


Figure S25. Steady state absorption spectrum of 8 in toluene.

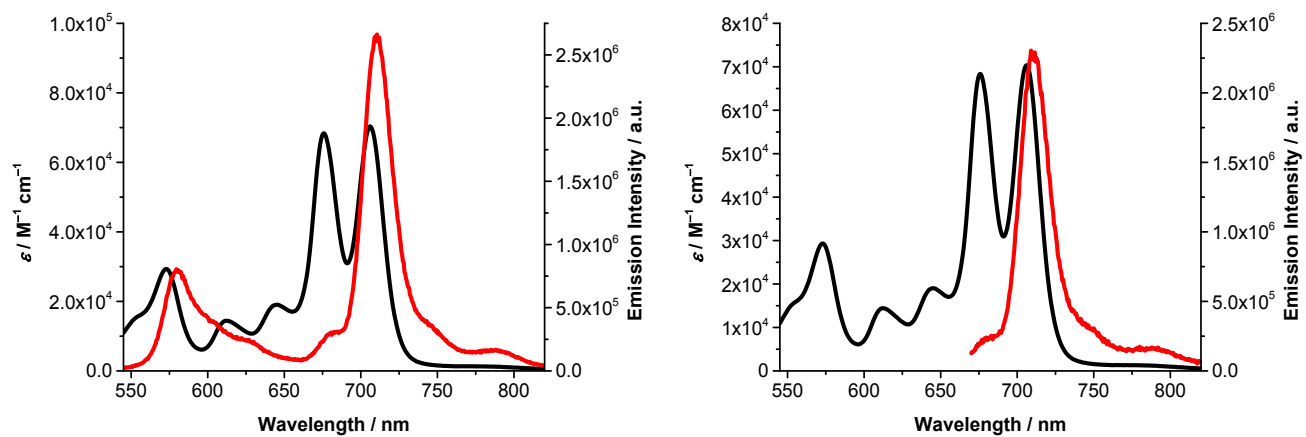


Figure S26. Steady state absorption (black) and fluorescence spectra (red) of **8** (1.42×10^{-6} M) recorded upon 530 excitation on the left and upon 655 nm excitation on the right in toluene.

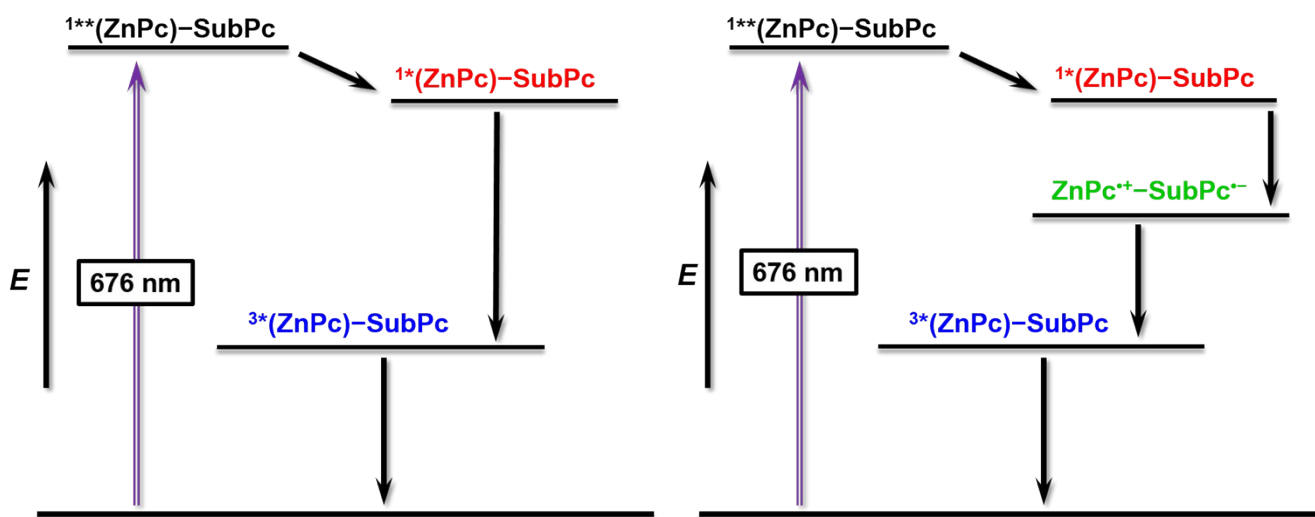


Figure S27. Three and four species energy level diagrams of ZnPc–SubPc **8** reflecting the energetic pathways in toluene (left) as well as anisole and benzonitrile (right) upon femtosecond flash photolysis (676 nm, purple arrow). Solid black arrows refer to nonradiative deactivation processes.

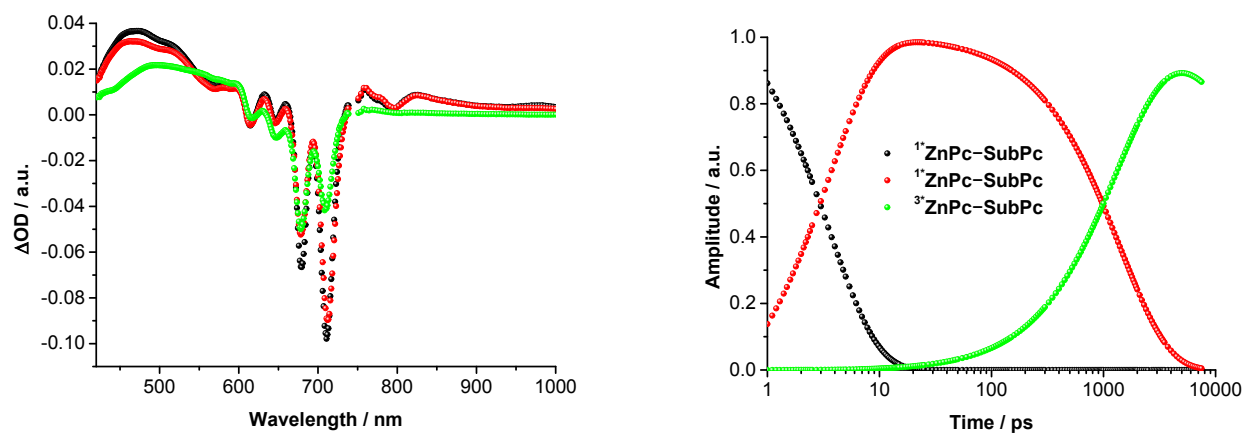


Figure S28. Evolution-associated transient absorption difference spectra (left) and associated time-dependent amplitudes (right) obtained upon femtosecond flash photolysis (676 nm, 200 nJ) of **8** ($2.5 \times 10^{-5} M$) in argon-saturated toluene.

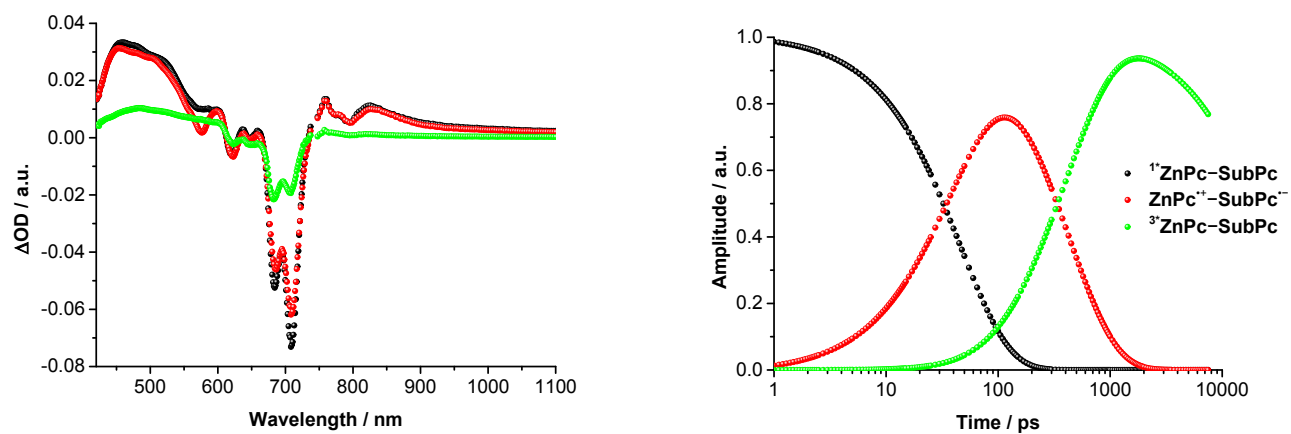


Figure S29. Evolution-associated transient absorption difference spectra (left) and associated time-dependent amplitudes (right) obtained upon femtosecond flash photolysis (676 nm, 200 nJ) of **8** (2.5×10^{-5} M) in argon-saturated benzonitrile.

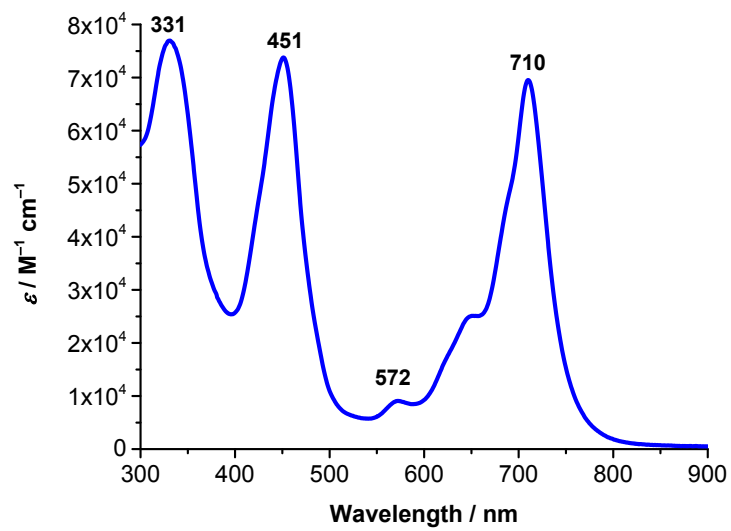


Figure S30. Steady state absorption spectrum of **9** in toluene.

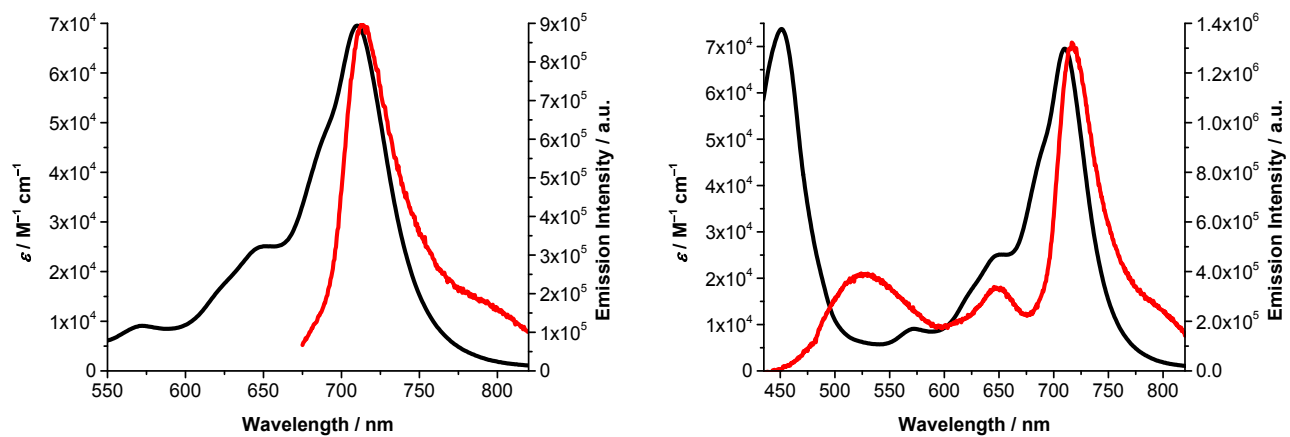


Figure S31. Steady state absorption (black) and fluorescence spectra (red) of **9** (1.09×10^{-6} M) recorded upon 660 excitation on the left and 420 excitation the left in toluene.

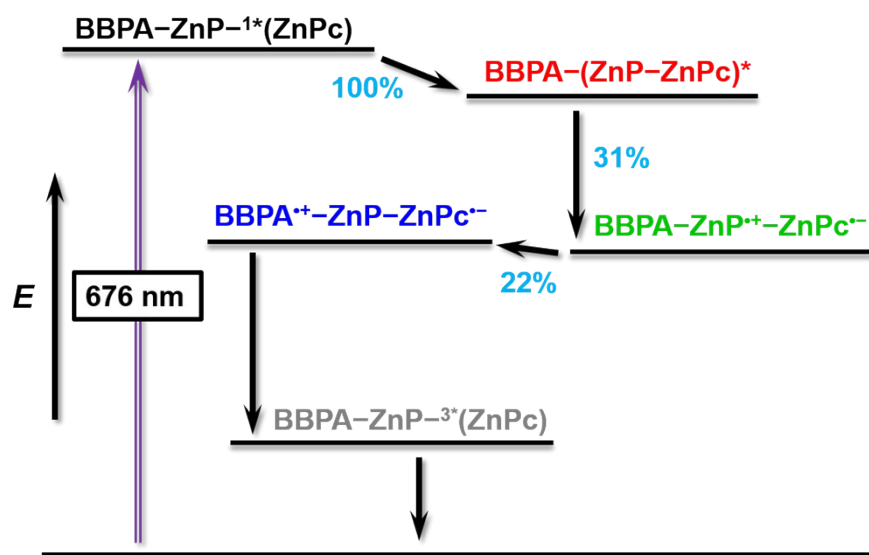


Figure S32. Four species energy level diagram of $(\text{BBPA})_3\text{-ZnP-ZnPc}$ **9** reflecting the energetic pathways in anisole upon femtosecond flash photolysis (676 nm, blue arrow). Solid black arrows refer to nonradiative deactivation processes and the numbers in blue to quantum efficiencies.

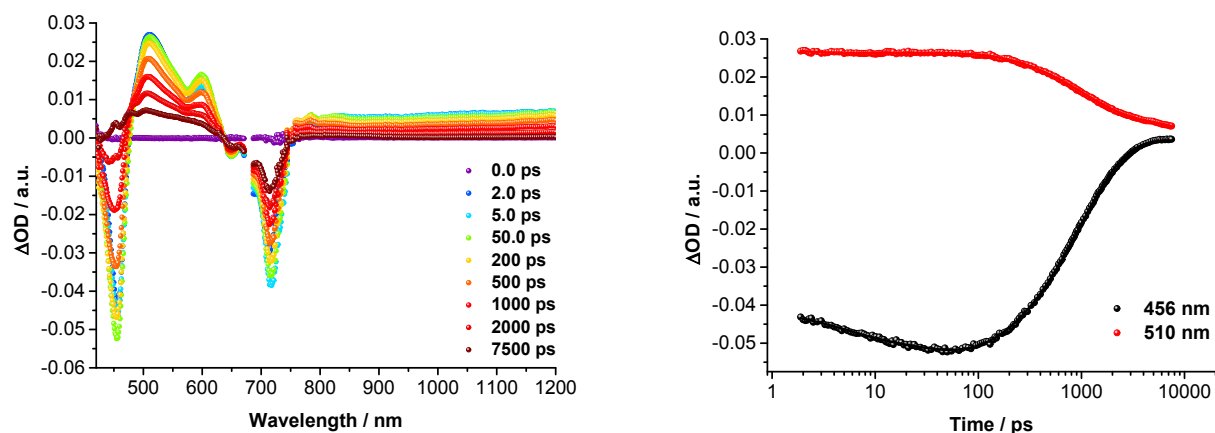


Figure S33. Differential absorption spectra (left) obtained upon femtosecond flash photolysis (676 nm, 200 nJ) of **9** (2.5×10^{-5} M) in argon-saturated toluene with several time delays between 0 and 7500 ps at room temperature; see legend for time evolution. Time absorption profiles (right) at 456 nm (black) and 510 nm (red) illustrating the excited state decay.

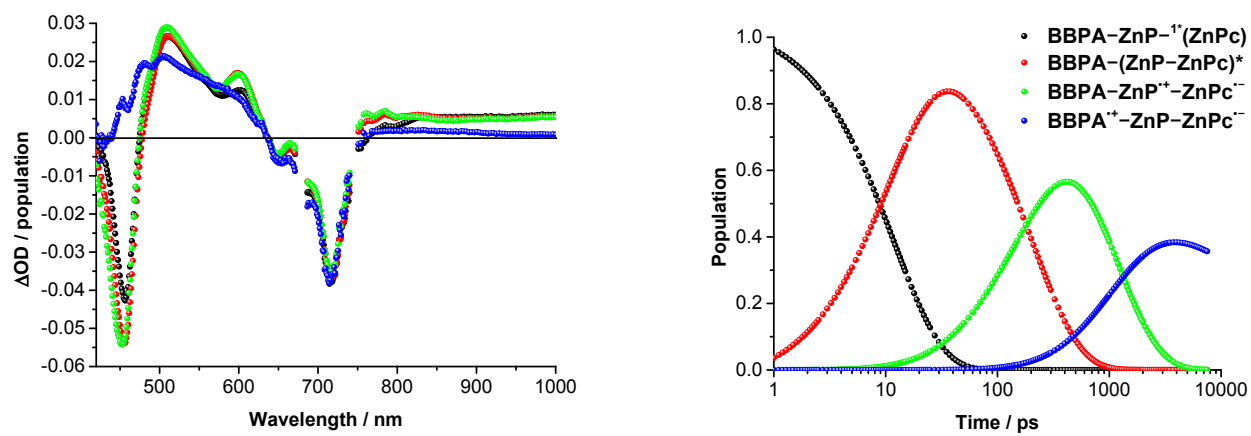


Figure S34. Species-associated transient absorption difference spectra (left) and population kinetics for each species (right) obtained upon femtosecond flash photolysis (676 nm, 200 nJ) of **9** (2.5×10^{-5} M) in argon-saturated toluene.

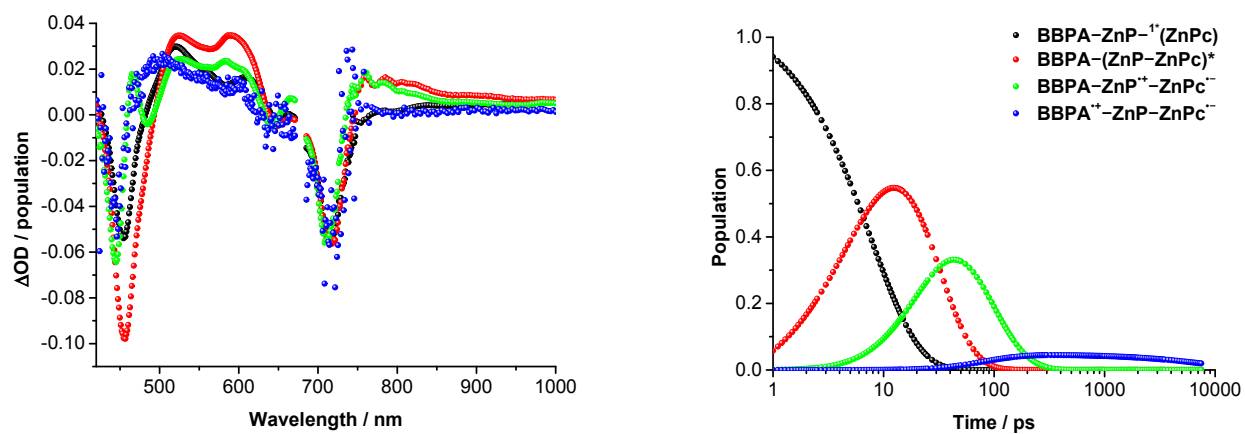


Figure S35. Species-associated transient absorption difference spectra (left) and population kinetics for each species (right) obtained upon femtosecond flash photolysis (676 nm, 200 nJ) of **9** (2.5×10^{-5} M) in argon-saturated benzonitrile.

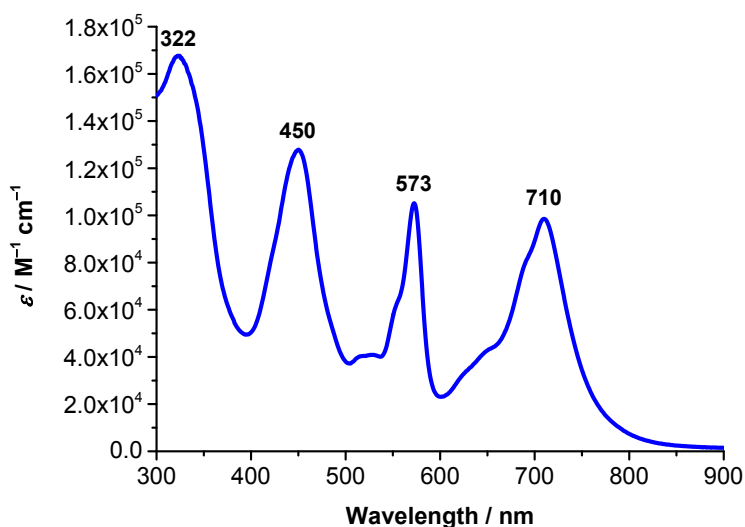


Figure S36. Steady state absorption spectrum of **1** in toluene.

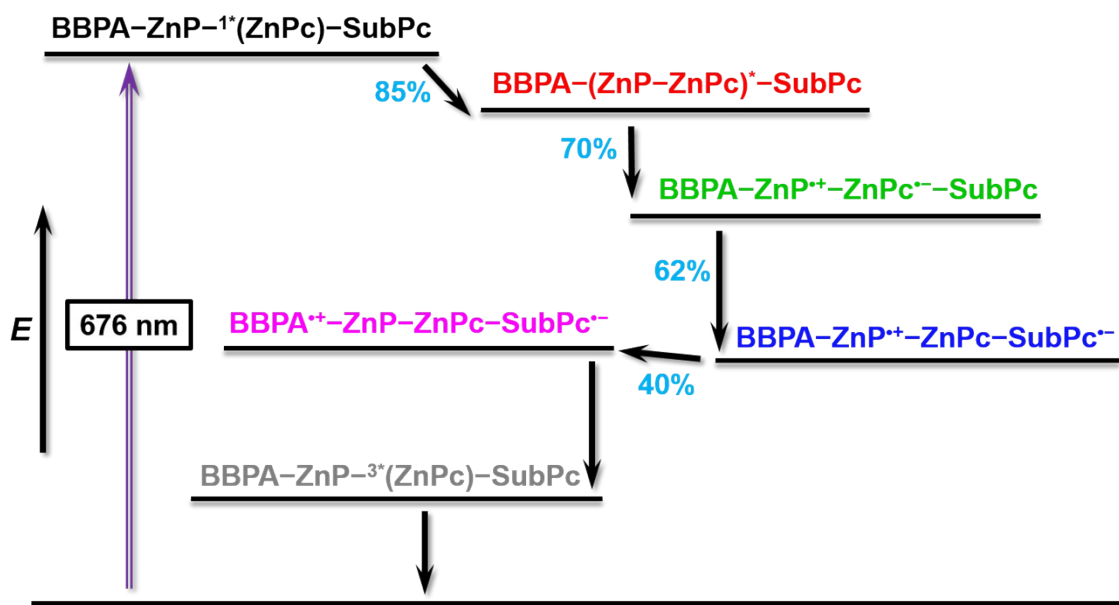


Figure S37. Five species energy level diagram of $(\text{BBPA})_3\text{-ZnPor-ZnPc-SubPc}$ **1** reflecting the energetic pathways in anisole upon femtosecond flash photolysis (676 nm, blue arrow). Solid black arrows refer to nonradiative deactivation processes and the numbers in blue to quantum efficiencies.

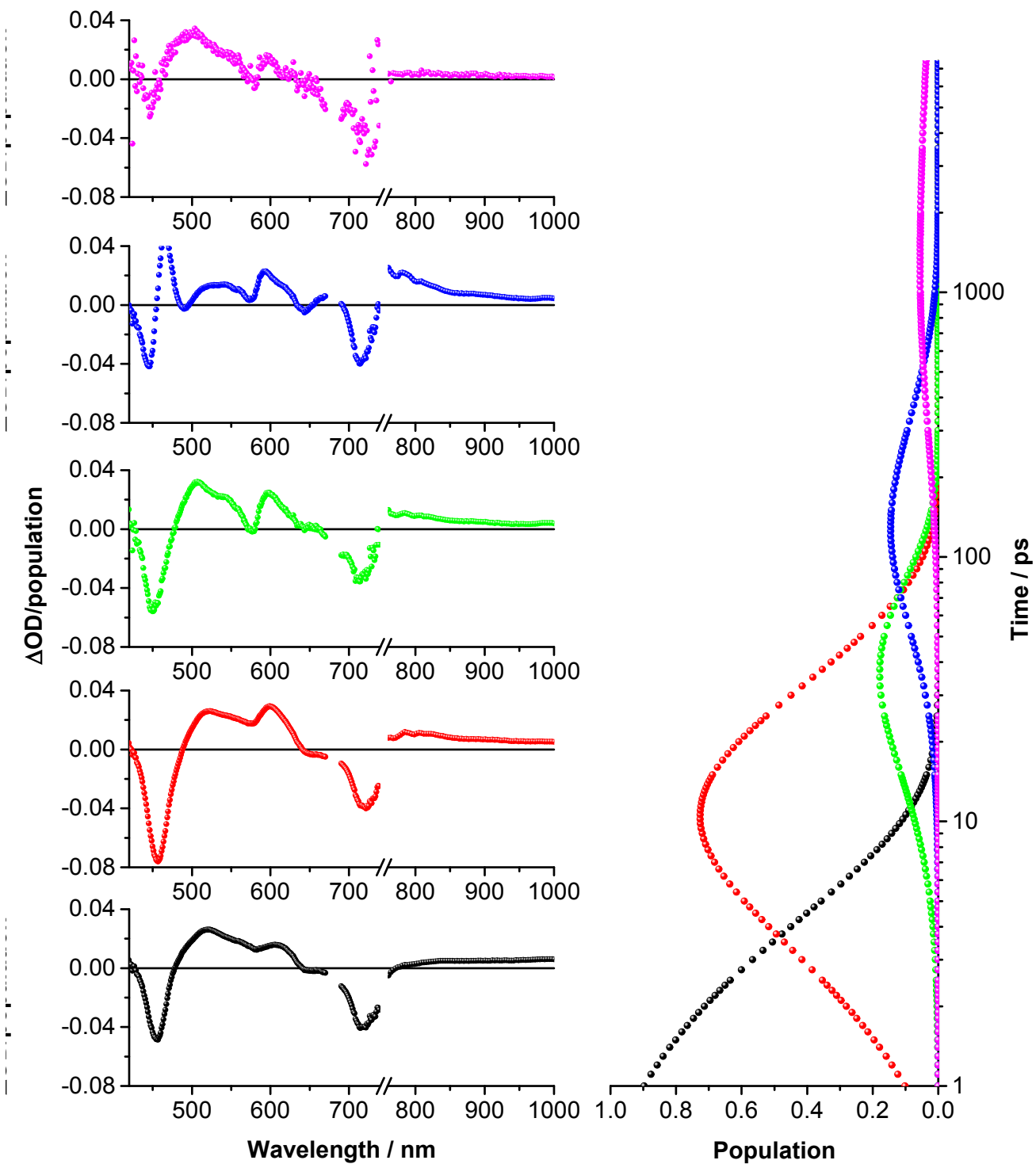


Figure S38. Left: Deconvoluted species-associated transient absorption difference spectra of $BBPA_3-ZnPor^{-1}*(ZnPc)-SubPc$ (black), $BBPA_3-(ZnPor-ZnPc)^*-SubPc$ (red), $BBPA_3-ZnPor^{*+}-ZnPc^{-}-SubPc$ (green), $BBPA_3-ZnPor^{*+}-ZnPc-SubPc^{-}$ (blue), and $BBPA_3^{+}-ZnPor-ZnPc-SubPc^{-}$ (magenta) for **1** ($2.5 \times 10^{-5} M$) as obtained by target analysis. Right: Population kinetics for each species. Data were obtained upon femtosecond flash photolysis (676 nm, 200 nJ) in argon-saturated benzonitrile.

- (1) Gao, P.; Kim, Y. J.; Yum, J.-H.; Holcombe, T. W.; Nazeeruddin, M. K.; Gratzel, M. *J. Mater. Chem. A* **2013**, *1* (18), 5535.
- (2) Claessens, C. G.; González-Rodríguez, D.; del Rey, B.; Torres, T.; Mark, G.; Schuchmann, H.-P.; von Sonntag, C.; MacDonald, J. G.; Nohr, R. S. *European J. Org. Chem.* **2003**, *2003* (14), 2547.
- (3) Fazio, E.; Jaramillo-García, J.; de la Torre, G.; Torres, T. *Org. Lett.* **2014**, *16*, 4706.